A MULTI-BAND POLARIZATION CONVERTOR WITH DUAL FUNCTIONALITIES BASED ON A ASYMMETRIC CRUCIFORM SHAPED METASURFACE AT TERAHERTZ FREQUENCY

A Project report submitted in partial fulfilment of the requirements for the award of the degree of

BACHELOR OF TECHNOLOGY

IN

ELECTRONICS AND COMMUNICATION ENGINEERING

Submitted by

B. Keerthi (319126512003)

K. Jyothir Sai (319126512022)

S. Ravi Teja (319126512052)

M. Surya Vamsi (319126512032)

Under the guidance of

Mrs. B. Rama Devi (Ph.D)

Assistant Professor

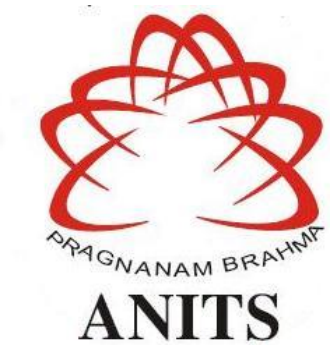

DEPARTMENT OF ELECTRONICS AND COMMUNICATION ENGINEERING

ANIL NEERUKONDA INSTITUTE OF TECHNOLOGY AND SCIENCES

(UGC AUTONOMOUS)

(Permanently Affiliated to AU, Approved by AICTE and Accredited by NBA & NAAC)

Sangivalasa, bheemili mandal, Visakhapatnam dist.(A.P)

2022-2023

DEPARTMENT OF ELECTRONICS AND COMMUNICATION ENGINEERING

ANIL NEERUKONDA INSTITUTE OF TECHNOLOGY AND SCIENCES

(UGC AUTONOMOUS)

(Permanently Affiliated to AU, Approved by AICTE and Accredited by NBA & NAAC)

Sangivalasa, Bheemili mandal, Visakhapatnam dist.(A.P)

PRAGNANAM BRAHMA

ANITS

CERTIFICATE

This is to certify that the project report entitled **"A MULTI-BAND POLARIZATION CONVERTOR WITH DUAL FUNCTIONALITIES BASED ON A ASYMMETRIC CRUCIFORM SHAPED METASURFACE AT TERAHERTZ FREQUENCY"** submitted by B.Keerthi(319126512003),K.Jyothir Sai(319126512022), S.RaviTeja(319126512052), M.Surya Vamsi (319126512032) in partial fulfillment of the requirements for the award of the degree of Bachelor of Technology in Electronics & Communication Engineering of Anil Neerukonda Institute of technology and Sciences(A), Visakhapatnam is a record of bonafide work carried out under my guidance and supervision.

Project Guide

Mrs. B. Rama Devi (Ph.D)

Assistant Professor

Department of ECE

ANITS

Assistant Professor
Department of E.C.E.
Anil Neerukonda
Institute of Technology & Sciences
Sangivalasa, Visakhapatnam-531 162

Head of the Department

Dr. B. Jagadeesh

Professor & HOD

Department of ECE

ANITS

Head of the Department
Department of E C E
Anil Neerukonda Institute of Technology & Sciences
Sangivalasa - 531 162

ACKNOWLEDGEMENT

We would like to like to express our deep gratitude to our project to our project guide **Mrs. B. Rama Devi (Ph.D)**, Assistant professor, Department of electronics and communication engineering ,ANITS, for his/her guidance with unsurpassed knowledge and immense encouragement . we are grateful to **Dr. B. Jagadeesh**, Head of the Department, Electronics and Communication Engineering, for providing us with the requirement facilities for the completion of project work.

We are very much thankful to the **Principal and Management, ANITS, Sangivalasa** , for their encouragement and cooperation to carry out this work.

We express our thanks to all **teaching faculty** of Department of ECE, whose suggestions during reviews helped us in accomplishment of our project. we would like to thank **all non-teaching staff** of the Department of ECE, ANITS for providing great assistance in accomplishment of our project.

We would like to thank our parents, friends, and classmates for their encouragement throughout our project period. At last, but not the least, we thank everyone for supporting us directly or indirectly in completing this project successfully.

PROJECT STUDENTS

B. Keerthi (319126512003)

K. Jyothir Sai (319126512022)

S. Ravi Teja (319126512052)

M. Surya Vamsi (319126512032)

CONTENTS

LIST OF FIGURES

LIST OF TABLES

LIST OF SYMBOLS

r_{xx}	Forward Reflection Coefficient
r_{yx}	Forward Transmission Coefficient
Er	The amplitude of the reflected wave
Ei	The amplitude of the transmitted wave
δ or $\Delta\Phi$	Phase Difference
Φ_x	Phase of Reflected wave
Φ_y	Phase of Transmitted wave

LIST OF ABBREVIATIONS

LCP	Linear Cross Polarization
LTCP	Linear to Circular Polarization
PCR	Polarization Conversion Ratio
EM	Electromagnetic
CST	Computer Simulation Technology
2-D	Two Dimensional
3-D	Three Dimensional

ABSTRACT

In this paper, the proposed is a terahertz wave polarization converter. The unit cell consists of cross shaped resonators. At the frequency bands 0.8726~0.8924 THz, 1.1075~1.1147 THz and 1.2614~1.2731 THz, the proposed metasurface behaves as linear to cross polarization converter with polarization conversion ratio more than 95% and ellipticity 0 for the reflected wave. It also behaves as linear to circular polarization converter at frequency bands of 0.516~0.862 THz, 0.947~0.986 THz and 1.986~1.203 THz. At these two frequency bands ellipticity of the reflected wave is in the range -1 to +1. Angular stability of the proposed metasurface is up to 50^{o} oblique incidence. Surface current distribution and multiple interference theory are used for analysing the root cause of polarization conversion. The simple structure, angular stability and dual functionality make the converter potential for the applications in terahertz detection, analysing the absorption spectrum of complex biological samples, as well as satellite communication.

Keywords— Terahertz, Metasurface, Polarization.

CHAPTER 1

INTRODUCTION

1.1 PROJECT OBJECTIVE:

Planar metamaterials known as metasurfaces are constructed from a two-dimensional array of subwavelength resonant or non-resonant unit cells. Polarization conversion is one of these metasurfaces' most important uses. In this light, different cross polarizers in the GHz and THz ranges have been reported. One of the most fundamental characteristics of EM waves is polarization. Several of these polarizers' designs are quite effective and broad-band. It is exceedingly challenging to convert linear to circular polarization over a wide-angle and wide-band simultaneously. Nonetheless, distinct designs for wide-angle and wideband circular polarizers have also been developed in the past. Designing a multifunctional metasurface with effective wide-angle, wideband linear, and circular polarization transformation is the major goal. It is a strong contender for many applications in the strategic for different bands due to its broad circular polarization conversion, compact size, angular stability, and numerous functionality.

1.2 METASURFACE DESCRIPTION:

Metasurfaces, which deal with subwavelength thickness, are two-dimensional (2D) or flat counterparts of metamaterials. Due to their special capacity to alter electromagnetic waves at microwave and optical frequencies, metasurfaces are employed in a variety of applications. Metasurfaces are composite material layers that are electrically thin and were specifically created and developed to act as a tool for the control and transformation of electromagnetic waves. Perfect absorption, anomalous reflection, focussing, and imaging are just a few of the many functionalities that metasurfaces have demonstrated strong capacities to achieve. Applications like electromagnetic cloaking, beam steering, and holographic displays are just a few examples of the numerous designs that have been developed that take advantage of this capability for a broad range of frequencies.

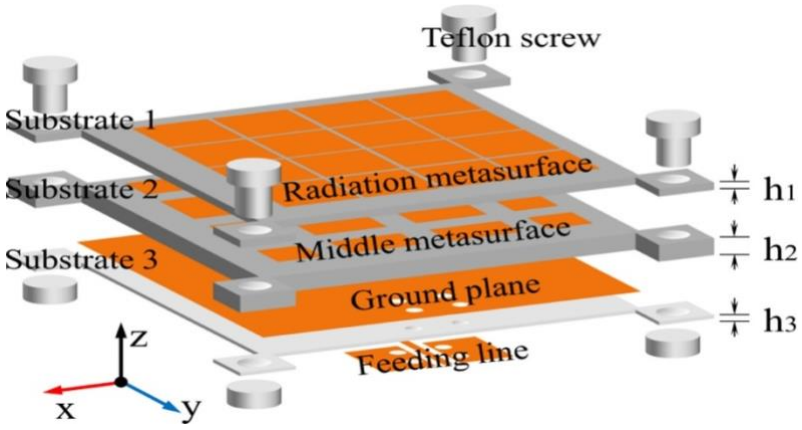

Fig.1.2 Low profile, broad band, double-layer metasurface microstrip antenna.

1.3 POLARIZATION IN METASURFACE:

Traditional optical elements like lenses and prisms can only control electromagnetic waves by accumulating phase delay during the process of light propagation, which severely restricts the size reduction and optical device integration. In wavefront modulation, amplitude and phase control are both very important. These conventional optical components are heavy for optical setup, as are diffractive components like gratings and holograms. In contrast, metasurface can more effectively achieve wavefront modulation by modifying the amplitude and imparting a sudden phase shift to the incident wave within the sub-wavelength scale through the interaction of light and matter. Several outstanding review studies have recently described the growth of this topic. Resonances with linearly polarised (LP) light, Panchanathan-Berry (PB) phase for circularly polarised (CP) light, and Huygens 'Principle with polarisation independence are the three major mechanisms for metasurface to alter the phase variation under specific polarisation states.

1.4TERAHERTZ TECHNOLOGY AND APPLICATIONS:

Recent developments in various fields of technology have opened up the hitherto untapped terahertz frequency region to imaging systems. In the electromagnetic spectrum, between microwave and infrared, there is a region known as the "terahertz gap" with frequency ranges between 0.3 and 10 THz. When compared to X-rays, terahertz radiations are innately harmless, non-destructive, and non-invasive because they are invisible to the naked eye. As this topic is so young, researchers from all over the world are competing to create the first usable system. It answers many of the issues that complementing methods like optical imaging, Raman, and infrared cannot.

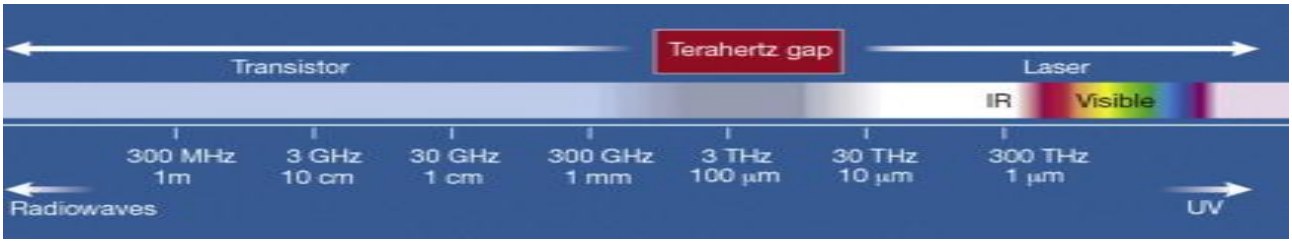

Fig.1.4 Terahertz frequency range.

Terahertz spectroscopy has a wide range of uses, including the detection of coating flaws in tablets, product inspection in industry, spectroscopy in chemistry and astronomy,

material characterization in physics, the detection of hidden weapons in clothing in airports, and the detection of cancer and tooth decay. It permits nondestructive internal chemical analysis of tablets, capsules, and other dosage forms in the pharmaceutical sectors. Hence, in addition to giving a brief review of imaging technology, this study also aims to cover the full spectrum of ongoing terahertz technology research and systems.

CHAPTER 2

PROBLEM IDENTIFICATION

2.1 PROBLEM IDENTIFICATION:

Several applications in the microwave and optical domains severely depend on the metasurface's capacity to sustain functioning for oblique incidence. With in mind, it is reported that double v-shaped and H-shaped metasurfaces function effectively as cross polarizers under oblique incidences.

1. The above metasurfaces perform only single operation that is crosspolarization conversion.
2. It is exceedingly challenging to achieve wide-band linear-cross polarization and wide-band linear to circular polarization conversion at the same time.

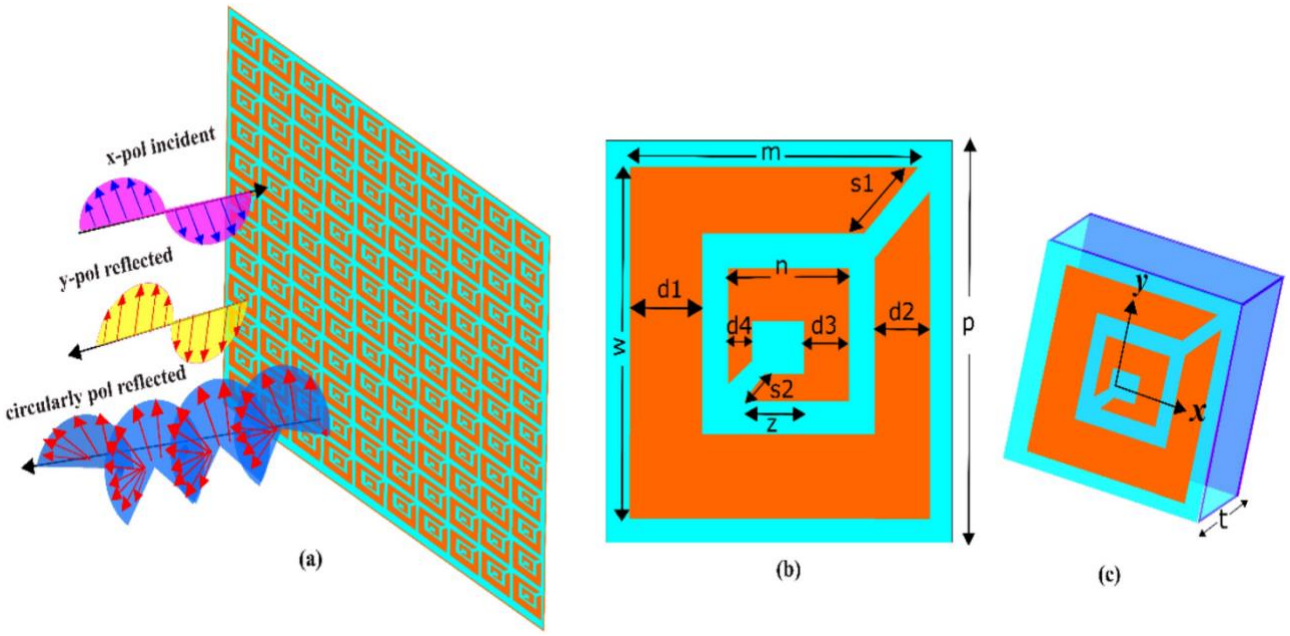

Fig.2.1 (a) A diagram showing the metasurface (b) Unit cell, (c) The unit cell in 3D.

Several applications call for various processes to be performed using a single metasurface architecture.

Hence, wideband linear to cross-polarization conversion and linear to circular polarization conversion are our key areas of interest. A multiband polarization converting metasurface is provided that converts linear to circular and circular to linear polarization in eight different frequency bands, as well as cross-polarization in five frequency bands. The structure's polarization changing capabilities span an extremely large frequency range (5-

37 GHz), including the majority of the X, C, Ku, K, and Ka bands. Several plasmonic resonances occuring in the device based on two connected rectangular split-ring resonators are the cause of this exceptional ultra-wideband performance. Moreover, for both

transverse-electric and transverse-magnetic polarizations, the polarization converting capability is stable over the frequency range 5–19 GHz at wide oblique incidence angles up to 60°. Additionally, the suggested structure functions as a meta-mirror to reflect light while maintaining the circular polarization's handedness. The findings of the numerical simulation are found to be congruent with measurements made on the manufactured metasurface. The proposed design qualifies as a prospective candidate for integration with significant microwave applications such as satellite, radar, and 5G communication due to its capacity to carry out three functionalities through a single small structure with outstanding bandwidth.

CHAPTER 3

METHODOLOGY

3.1 METHODOLOGY:

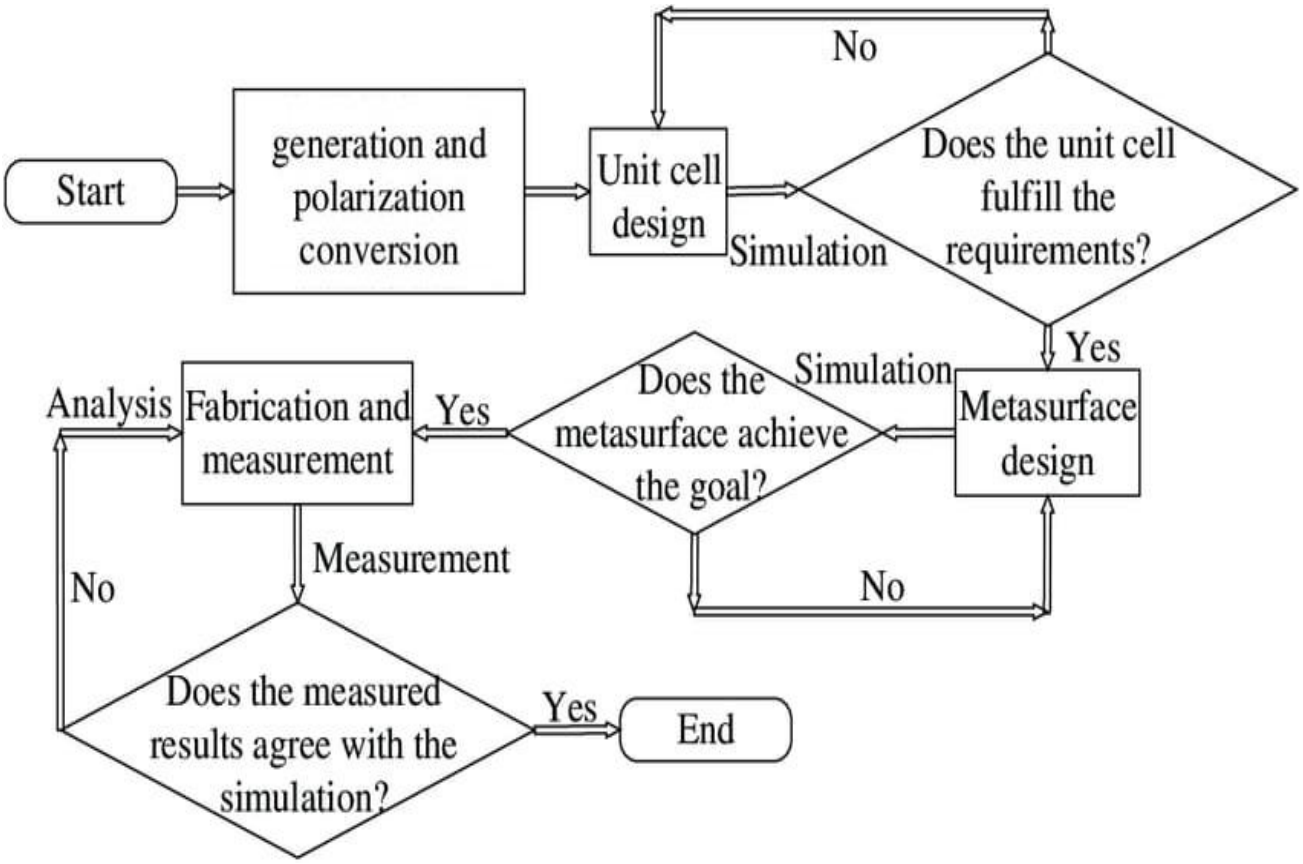

CHAPTER 4

METASURFACES

4.1 INTRODUCTION TO METASURFACES:

Metasurfaces are the two-dimensional (2D) or flat equivalents of metamaterials, which deal with subwavelength thickness. Metasurfaces have the rare capacity to block, absorb, concentrate, scatter, or steer waves in space at normal and oblique incidence as well as on the surface at grazing incidence angles, from microwave to visible frequencies. Surface waves may be efficiently managed by designing impedance cells to adjust group velocity or phase. They are built with the capacity to regulate dispersion, as well as to separate or steer waves in certain directions. By altering the metasurface, unit cell sizes, and shapes, a variety of effective surface refractive indices and functions may be produced. For 2D microwave/optical antenna systems, planar microwave sources, and Luneburg and fish-eye lenses.

Humans produce metamaterials, which contain different spatial modifications in their constituent elements. They are widely used to modify a material's elastic, electromagnetic, or acoustic characteristics. Metamaterials provide low/high-frequency band gaps to control wave propagations with different wavelengths in addition to being often utilised in microwave engineering, waveguides, dispersion correction, smart antennas, and lenses. Permittivity and permeability of the metamaterials, for example, may have positive or negative values. In order to guide waves, surface-based metamaterials are used since their single-cell dimensions are less than their wavelength. The need for tunable bandgaps may also motivate research into the tunability of metamaterials for structures that function at varying speeds. This article reviews the most current research on metamaterials and its applications. The piezoelectric and electromagnetic metamaterials are presented after a summary of innovative chiral metamaterial types. In addition, comparisons between absorber, nonlinear, terahertz, tunable, photonic, selective surface-based frequency in acoustic metamaterials are provided. Also, some remarks are given on tuning bandgaps procedures in locally resonant metamaterials.

Narrowband, broadband, and wideband metasurface-based devices have been classified based on the materials used, their geometry, and their frequency responses. Fano resonance is the usual application for narrowband technology. The abrupt resonant peak of the Fano resonance, which is followed by a significant local field rise, is one of its fundamental properties. It serves as the foundation for a variety of practical applications, such as nonlinear photonics and biological sensing. High-performance colour filters, broadband absorbers, and polarizers, as well as super-resolution imaging beyond the diffraction limit, may all be supported by metasurface dispersion for multiband and broadband applications.

4.2 TYPES OF METASURFACES:

Narrowband, broadband, and wideband metasurface-based devices have been classified based on the materials used, their geometry, and their frequency responses. Fano resonance is the usual application for narrowband technology. Fanoresonance has a strong resonance peak and a significant local field augmentation as one of its primary properties. It serves as the foundation for a variety of practical applications, such as nonlinear photonics and biological sensing. High-performance colour filters, broadband absorbers, and polarizers, as well as super-resolution imaging beyond the diffraction limit, may all be supported by metasurface dispersion for multiband and broadband applications.

Metasurfaces are two-dimensional (2D) or planar variations of metamaterials when dealing with subwavelength thickness. Metasurfaces have the specialised capacity to block, absorb, concentrate, scatter, or steer waves at frequencies spanning from microwave to visible when incident in space at normal and oblique angles as well as on the surface when incident at grazing incidence angles. Surface waves may be effectively manipulated by constructing impedance cells to alter group velocity or phase. They are made with the ability to regulate dispersion, separate waves, or guide waves in certain directions. By adjusting the metasurface, unit cell sizes, and shapes, different functions may be imprinted on the surface, and different effective surface refractive indices can be created. They may be used to create 2D fish-eye and Luneburg lenses, as well as other optical and microwave components, for antenna systems and planar microwave sources.

Metamaterials are made by people and feature different spatial modifications in their fundamental components. They are widely used to alter the elastic, electromagnetic, or acoustic characteristics of materials. Metamaterials are often used in microwave engineering, waveguides, dispersion correction, smart antennas, and lenses, but they also provide low/high-frequency band gaps that control wave propagation over a range of wavelengths. For example, the permittivity and permeability of the metamaterials may have positive or negative values. As their single-cell dimensions are less than their wavelength, surface-based metamaterials are used for waveguiding. The need for changeable bandgaps may also serve as a catalyst for research into the tunability of metamaterials for structures operating at varying speeds. In this article, the most current metamaterials research is covered along with its applications. The introduction of piezoelectric and electromagnetic metamaterials follows a summary of innovative chiral metamaterial types. Acoustic metamaterials' absorber, nonlinear, terahertz, adjustable, photonic, and selective surface-based frequency are also contrasted. Moreover, some suggestions on how to adjust bandgaps in locally resonant metamaterials are given.

a discussion of a

4.2.1Gap-Plasmon Metasurfaces:

Reflective-array metasurfaces, which utilise the metal-insulator-metal structure as its core building block, are created by adding a dielectric spacer and a metallic ground sheet below metallic antenna arrays. The optically thin dielectric layer exhibits a strong near-field interaction with the top antenna array and its mirror dipoles in the metallic plane, which enables a two phase modulation. The ground plane and Nano antennas' antiparallel generated currents on the gap-surface Plasmon modes, which generate a strong magnetic field within the insulator. [25, 26] Nano rod antennas and H-shaped antennas, which function in the near-infrared and microwave domains, respectively, are shown in Figures 2d and 2e. The radiation phase may be successfully changed by simply changing the antenna length. [26–30]

As the reflected amplitude does not considerably differ across unit structures at the design stage, one may just focus on phase response during this time. The inhibition of transmission by the metallic ground plane allows for conversion efficiency to the anomalous reflection mode to reach up to 80%. [21] Also, this technique has the desirable property of retaining the polarisation state of the incident wave in the reflected wave.

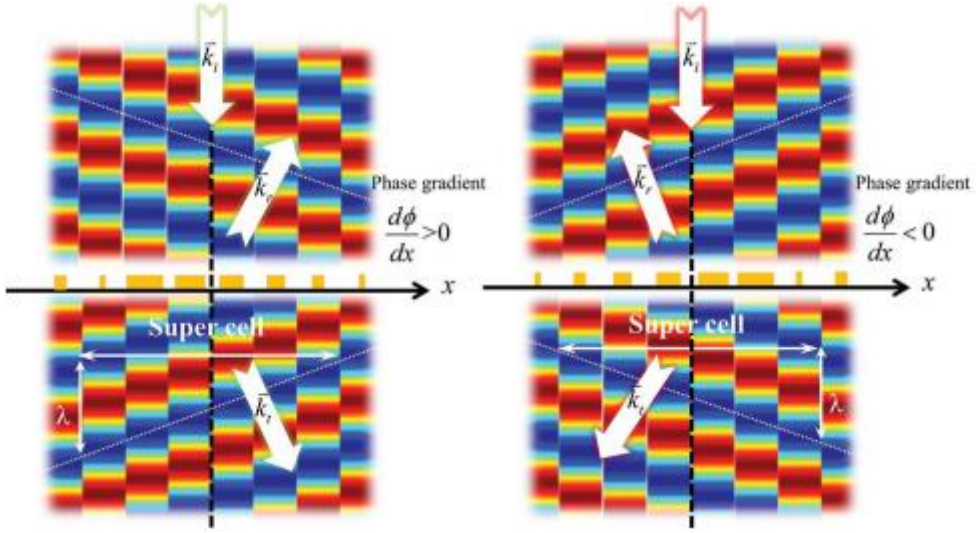

Fig.4.2.1 Gap-Plasmon Metasuraces.

4.2.2 Multi-Resonance Metasurfaces:

Two Nano rods of the same length joined at an angle to form V-shaped antennas, which were the first proposed nanostructures with a phase variation of 0 to 2. The two resonant modes that this plasmatic antenna supports may be divided into symmetric and antisymmetric modes based on their current distributions (Figure 4.2.1). [5,18]

The symmetric (antisymmetric) mode is excited when the polarisation of the incoming electric field (Einc) is parallel or perpendicular to the antenna's symmetry axis. When the incident wave is neither parallel to the antenna symmetry axis nor perpendicular to it, both resonant modes may be engaged concurrently. The hybridization of two Eigen modes results in the generation of two polarisation states in dispersed radiation: [19] One is (2β – α)-polarized and is attributed to anomalous components, where is the angle formed by the y coordinate and the antenna symmetry axis. (Capasso and colleagues[19] discuss the physics of the V-shaped antenna and its analytical model in considerable detail.) The cross-polarized scattered light (2β – α= 90° or 0°) can have a wide range of phases and amplitudes by varying the antenna geometry and orientations, as first demonstrated by Yu et al. in the mid-infrared[5] and later demonstrated by Ni et al. in the near-infrared[20]. This is possible by correctly selecting β = 45° and α = 0° or 90°. However, since normal and anomalous reflection/refraction coexist in this process, the efficiency of the intended light-manipulation effect is very constrained. Also, since they vary in polarisation from the incoming light, the use of anomalously reflected or refracted optical beams is constrained.

Table 1. The unique properties of six categorized metasurfaces.

	Multi-resonance metasurfaces	Gap-plasmon metasurfaces	PB-phase metasurfaces	Huygens' metasurfaces	All-dielectric Huygens' metasurfaces/high-contrast metasurfaces
Outstanding Properties	• First proposed structures	• High efficiency • Co-polarized conversion	• Easy design • Broadband • Large fabrication tolerance	• High transmittance efficiency in the microwave and near-infrared regimes	• Low absorption loss at optical frequencies • High transmission efficiency
Limitations	• Low efficiency • Cross-polarized conversion	• Limited to reflective applications	• Limited to circularly polarized light operation	• Require multi-layered structures • Degrading performance in the optical regime	• Limited operation bandwidth in the visible • Limited choices of materials

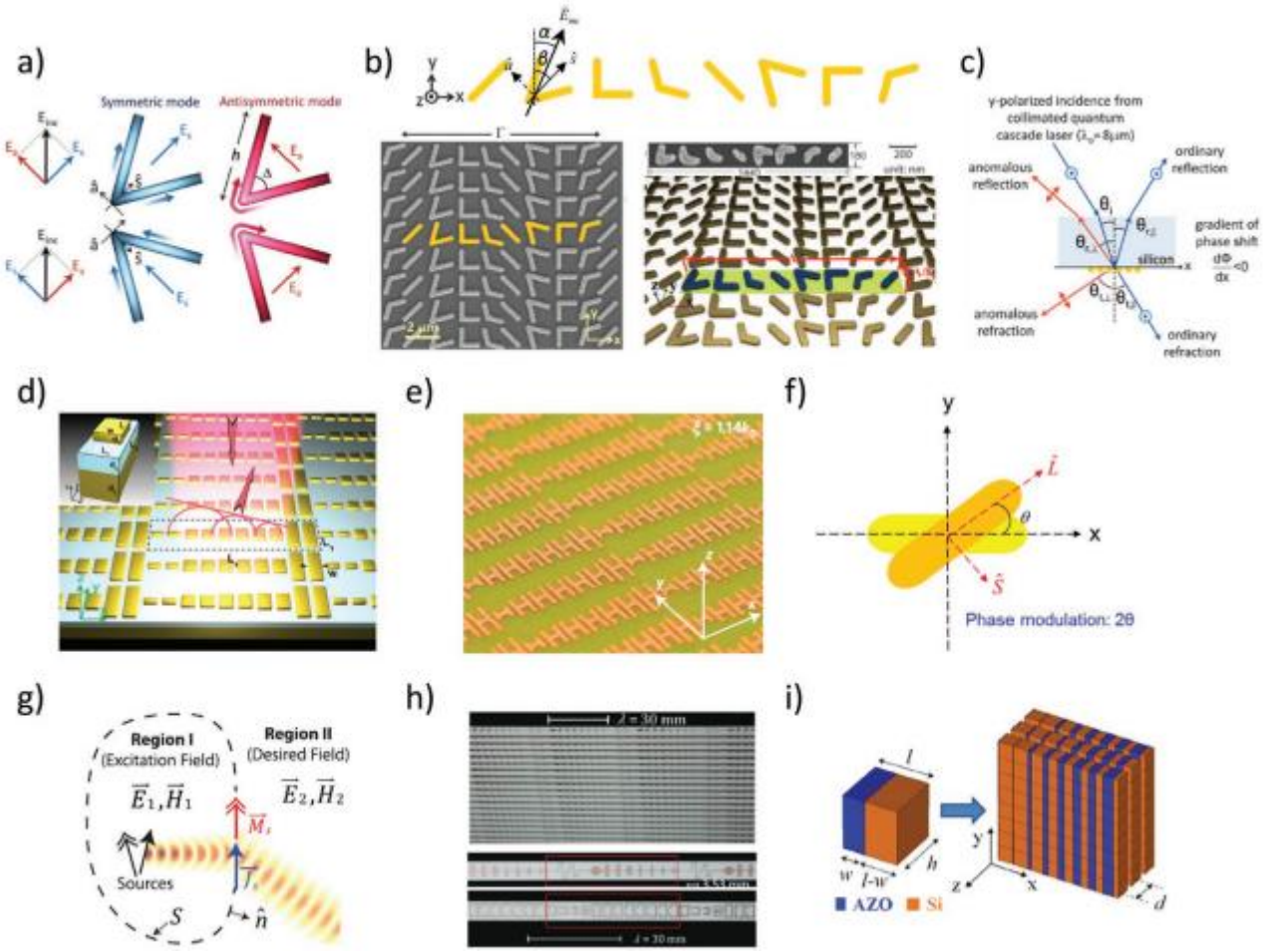

Fig.4.2.2 Multi-Resonance Metasurfaces.

4.2.3 Panchanathan–Berry-Phase

Full phase control is accomplished using a separate technique known as Panchanathan-Berry-phase (PB phase) metasurfaces by altering the orientation angle of antennas with comparable shape. Metasurfaces Variations in antenna geometry are the basis for changes in the phase or amplitude of the aforementioned metasurfaces. [31,32] and and represent the complex transmission coefficients of an anisotropic nanostructure under normal incidence, respectively, where the polarisation of incoming light is along the two major axes of the nanostructure. As the Nano resonator is rotated an angle from the x axis, it is possible to calculate the transmission coefficients for this revolving system using the Jones matrix operation.

$$\hat{t}(\theta) = R(-\theta)\begin{pmatrix} t_0 & 0 \\ 0 & t_e \end{pmatrix}R(\theta)$$

$$= \begin{bmatrix} \cos\theta & -\sin\theta \\ \sin\theta & \cos\theta \end{bmatrix}\begin{bmatrix} t_0 & 0 \\ 0 & t_e \end{bmatrix}\begin{bmatrix} \cos\theta & \sin\theta \\ -\sin\theta & \cos\theta \end{bmatrix}$$

$$= \begin{bmatrix} t_0\cos^2\theta + t_e\sin^2\theta & (t_0 - t_e)\cos\theta\sin\theta \\ (t_0 - t_e)\cos\theta\sin\theta & t_0\sin^2\theta + t_e\cos^2\theta \end{bmatrix}$$

Where R(θ) is the rotation matrix. When the incident wave is circularly polarized (CP), the transmitted electric field (EL/R t) can be derived by applying matrix multiplication of Equation (2) and the Jones' vectors of left-handed CP (LCP) or right-handed CP (RCP) light e e ˆL/R = ± (ˆ ˆ x y ie)/ 2 and written as

$$E^t_{L/R} = \hat{t}(\theta)\cdot\hat{e}_{L/R} = \frac{t_0 + t_e}{2}\hat{e}_{L/R} + \frac{t_0 - t_e}{2}e^{\pm i2\theta}\hat{e}_{R/L}$$

The first component of equation (3) refers to CP scattered waves that have the same helicity as the incident wave, whereas the second term refers to CP scattered waves that include an extra Panchanathan-Berry phase and have the opposite helicity (i2). As a result, a phase shift from 0 to 2 may be established for radiation of the opposite handedness when the nanoresonator is spun from 0 to. Since it employs orientated clones of a single antenna design for phase modulation, this method has the benefit of being straightforward to design, having a larger manufacturing tolerance, and being beneficial for broadband applications.

4.2.4 Huygens' Metasurfaces

Because the performance of transmitted-type metasurfaces is severely hampered by the insufficient coupling efficiency of single-layered plasmonic antennas to the phase-controlled mode, an alternative method based on the surface equivalence principle was proposed to reduce reflection by concurrently adjusting the electric and magnetic polarizabilities at the interface. The requisite field distributions are produced by surface electric and magnetic currents (s J - and M s -) at two places with different electromagnetic characteristics.

$$\vec{J}_s = \hat{n} \times \left(\vec{H}_2 - \vec{H}_1\right), \quad \vec{M}_s = -\hat{n} \times \left(\vec{E}_2 - \vec{E}_1\right)$$

In order to construct surface impedances locally, Huygens' metasurface designs may use nonperiodic or multilayered structures. The following relation should be met at the interface in order to rectify field discontinuities using any arbitrary waveform for both the intended and impinging waves. For instance, Pfeiffer and Grbic used a supercell with 12 patterned parts to build a beam deflector in the microwave regime with 86% transmittance. [23] Monticone et al. reported a stack of three-layered metasurfaces for light bending in the near-infrared region with a theoretical efficiency of 75% produced from a mix of dielectric and plasmonic nanoblocks functionalized as nanoinductors and capacitors, respectively. [24]

Huygens' metasurfaces perform much worse at optical frequencies, with a proven efficiency that stays below 20%. [38] This is caused by the natural materials' subpar magnetic response and the intrinsically metallic loss of plasmonic components in the visible range.

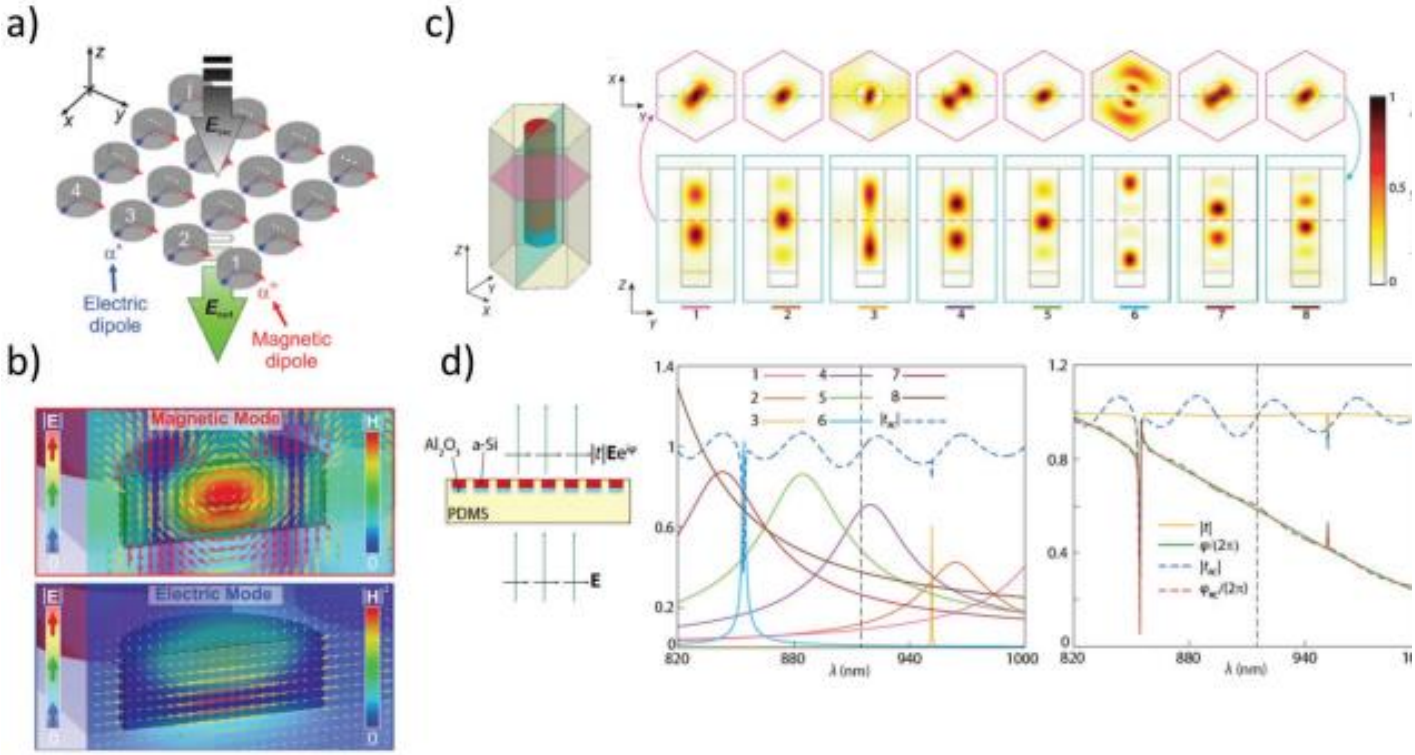

Fig.4.2.4 Huygens' Metasurfaces.

4.2.5 All-Dielectric Huygens' Metasurfaces:

Plasmonic metasurfaces suffer from increasing dissipative losses at optical frequencies as well as a number of unfavourable loss channels that occur during the phase-modulation process, such as diffraction, regular reflection/refraction, and polarisation conversion losses. This opens up a new area of research focused on the dielectric analogues of metasurfaces. It was found that the highest transmitting efficiency with the Huygens' metasurfaces requires the production of electric and magnetic resonances with comparable intensities that are spectrally overlapping by high-refractive-index dielectric nanoparticles or nano discs. On the other hand, owing to their low inherent losses, dielectric nanoparticles may couple the incoming wave to produce circular displacement currents within the nanostructures and give rise to a strong magnetic dipole resonance (Figure 3a,b). In contrast, the significant metallic losses at visible frequencies in their metallic counterparts result in disappearing fields within nanoparticles and a minimal magnetic response as a result. For instance, employing arrays of high-permittivity silicon (Si) nanodisks, Kivshar's team showed a 0-to-2 phase coverage with a transmission efficiency of more than 55% in the near-infrared region. [40] Also shown was an all-dielectric Huygens' metasurface-based beam deflector with a potential efficiency of up to 45% at visible frequencies.

4.2.6 High-Contrast Metasurfaces:

Simultaneous phase and polarisation control with strong transmission is another capability of high-contrast metasurfaces. Dispersed high-refractive-index dielectric scatterers placed into a periodic 2D lattice make up these metasurfaces. A variety of low-quality Fabry-Perot resonances are supported by a variety of nanoscatterers, each of which may be conceptualised as a single truncated waveguide. Electric and magnetic dipoles, quadrupoles, and higher-order multiples are the resonant modes of high-contrast metasurfaces, as opposed to magnetic dipole resonances. [47] Due to the large difference in refractive indices between the nano scatterers and their surroundings, the geometry of the nano scatterers determines the transmittance property more so than the optical coupling between them, which has little to no effect. High contrast metal surfaces have been proven to act as polarisation beam splitters, with observed transmission efficiencies of higher than 70% for both x- and y-polarized light.

CHAPTER 5

LITERATURE SURVEY

Table 1

Analyzing the proposed structure in light of previous converters that have been described.

References	Year	Polarization properties	Operation Frequency	Eilli.	PCR	Angular stability
Pan W [17]	2018	Cross	0.58~1.35 THz	NIL	85%	30˚
Jiang Y [16]	2017	Circular	0.60~1.41 THz	0.8	NIL	20˚
Dutta R [27]	2021	Cross Circular	4.3,7.2,12.3,15.15 GHz 4.75~5.95, 8.35~8.8 GHz	NIL 0.9	90% NIL	15˚
Bilal H [30]	2020	Cross Circular	1.10,2.13,3.46 THz 1.20~1.83,2.52~3.10, 3.78~3.90 THz	NIL 0.8	90% NIL	20˚
This work	2023	Cross Circular	0.87~0.89,1.10~1.11,1.26~1.27THz 0.51~0.866,0.94~0.98,1.98~1.20THz	NIL 0.96	95% NIL	50˚

The focus of recent terahertz polarization conversion research has been on the operational bandwidth, PCR, and ellipticity of the resultant circularly polarized waves. For instance, Wen X et al. [12] developed a converter with a narrow bandwidth in 2014. The converter achieved LCP conversion in the frequency range of 0.44~0.76 THz, with a PCR of over 80%. In order to achieve the broad operating band LCP conversion, Pan W et al. [13] integrated a split resonant ring and a hollowed-out disc on a metasurface in 2018. The PCR was higher than 85% in the frequency range of 0.584~1.352 THz. In 2021, Cao T N et al. [14] used a variety of resonator shapes to produce a single-layer metasurface LCP converter with a PCR of more than 90% in the 1.35~3.55 THz frequency range. It was also proposed that the LTCP converters function in THz. Thanks to a terahertz LTCP converter developed by Wang D et al. in 2015 [15], the ellipticity of the resulting circularly polarized waves was 0.9 in a condensed bandwidth. In 2017, Jiang Y et al. [16] developed a metasurface structure using a double split resonant ring structure that produced LTCP conversion within the range of 0.60–1.41 THz and had an ellipticity of circularly polarized waves that was close to 0.8. With an ellipticity of 0.8, the LTCP conversion in the 0.60~0.85 THz band must be accomplished. A structure based on a broken line metasurface was suggested by Pan W et al. [17] in 2019. The interaction of active

materials with the metasurface is the main topic of study for the polarization converter. There have recently been many converters created using active materials including graphene, vanadium dioxide, and photosensitive silicon. The function transitions of LCP conversion to absorption [18–20], transmission to reflection mode [21–23], and LCP to LTCP [24] are all accomplished by these converters. While active material-based metasurface converters may switch between functions with flexibility, they nevertheless have significant production costs and are unable to directly integrate several functionalities. Polarization converters with several bands and functionalities, as was previously mentioned, provide a broad variety of possible applications. Thanks to Khan M I et al. [25], multiband LCP and LTCP conversion in microwave frequency was made possible by metasurface in 2019. A dual-band converter that can perform LCP and LTCP conversion in the ranges of 7.74~14.44 GHz and 14.95~17.35 GHz was presented in 2020 by Zheng Q et al. [26]. Dutta R et al. introduced a meandering square metasurface converter in 2021 [27] to achieve LCP and LTCP conversion at microwave frequency, despite the fact that the stability of the oblique incidence angle can only reach 15. A butterfly-shaped ultra-thin multifunction converter that can perform LCP and LTCP conversion in two microwave frequencies was developed in 2022 by Hao F et al. [28]. The converter is stable up to a 30° oblique incidence angle. In the terahertz frequency range, research on multi-function and multi-band polarization converters has been ongoing. A bi-layered subwavelength metal grating sandwiched between a symmetrical dual radar structure array was used in the dual-band converter Li J S et al. [29] created in 2020 to achieve LCP conversion at 0.38~1.34 THz and 1.40~2.23 THz with a PCR of more than 95%. In the same year, Bilal R M H et al. [30] developed a complicated fractal metasurface structure that experienced LTCP conversion at 1.20 THz, 1.83 THz, 2.52 THz, and 3.78 THz in addition to LCP conversion at 1.10 THz, 2.13 THz, and 3.46 THz. The converter exhibited an angular stability of up to 20°, and the generated circularly polarized waves had an elasticity of about 0.8. In 2022, Luo H et al. introduced an all-metal stereo structure anisotropic metasurface-based dual-functional polarization converter [31]. The simulation's results show that the converter can convert at 1.45 THz for LCP and at 1.37 and 1.54 THz for LTCP. The incidence angle stability of the converter was close to 50 degrees. Despite the fact that the aforementioned multi-band and multi-functional polarization converters improve polarization conversion function, they also have some drawbacks, such as low elasticity of the obtained circularly polarized wave, a narrow LTCP conversion band, a complex design structure, poor stability of incident angular, and others.

CHAPTER 6

CST TOOL

6.1 CST TOOL

6.1.1 3D EM Technology

CST Microwave Studio offers quick and precise 3D EM simulation tools for **high frequency** issues. It provides a wide range of various solvers that operate in the time and frequency domains.

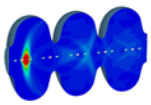

Simulating **static and low frequency** issues in 3D EM with CST EM Studio. The module offers a substantial selection of solvers for numerous applications.

CST Particle Studio: Specialized solvers for the three-dimensional (3D) simulation of charged **particle interactions with electromagnetic** fields. The software has a variety of solvers that deal with these difficult situations.

6.1.2 SPARK3D:

Radio frequency (RF) breakdown analysis software in general. It employs strong and precise numerical methods to forecast the onsets of corona (arcing) and multipactor breakdown, two of the key high power phenomena that can seriously harm a device.

6.1.3 FEST3D:

A powerful software tool for the precise study of waveguide-based passive components.

The first commercial software that can incorporate high power effects during the design phase is called FEST3D.

6.2 Cable | Circuit | Macromodels | PCB | Chip

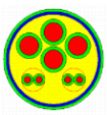

The CST Cable Studio provides tools for analysing SI, EMC, and EMI effects in cable systems, including those with single wires, twisted pairs, and intricate cable harnesses.

6.2.1 CST Design Studio:

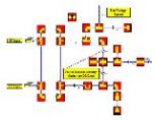

A tool for system level simulation design and analysis. The connecting of several 3D projects and circuit elements is made possible by its schematic perspective. It serves as the starting point for our potent circuit simulator and the System Assembly and Modeling (SAM) procedures.

A tool called IDEM is used to create macromodels of electrical interconnect architectures that are SPICE-ready. IdEM offers precise, validated, passive, and causal broadband computational models that may be applied in any circuit modelling environment starting with their input-output port responses.

6.2.2 CST PCB Studio:

Tools for the design of 3D chips, the analysis of signal and power integrity, and the simulation of EMC and EMI effects on printed circuit boards (PCBs).

6.2.3 CST MPhysics Studio:

A collection of instruments for addressing both thermal and mechanical stress issues. To address coupled simulation tasks, use these solutions in conjunction with other simulation domains.

6.3 Installation:

CST Studio Suite can be easily installed. You may learn everything you need to know about installation in this chapter. The following sections are covered:

- Installation requirements
- Licensing options
- Installation instructions for Microsoft Windows
- License Server
- Starting CST Studio Suite

Please note:

The installation on a Microsoft Windows operating system is the subject of this document. Please refer to the documentation included with the Linux package to install the software on Linux.

6.3.1 Installation Requirements:

6.3.1.1 Software Requirements:

Windows 7 with Service Pack 1 or later, Windows 2008 Server R2 with Service Pack 1 or later, Windows 8.1, Windows 2012 Server R2, Windows 10, Windows Server 2016, and Windows Server 2019 are all compatible with the programme.

6.3.1.2 Hardware Requirements:

- IBM PC compatible CPU (Intel Xeon processor strongly recommended)
- OpenGL compatible graphics hardware
- 4 GB RAM (8 GB recommended)
- 30 GB free disk space (60 GB recommended)

6.3.2 Licensing Options:

Either a network version or a single PC (node locked) version of the software can be licenced. The software may only be used on a single PC with a single PC licence. In contrast, a network licence enables the software to be used across many PCs that are linked to a licence server.

With both types of licences, the installation process largely consists of the same steps. So, we will first concentrate on the standard practises before outlining the variations in licence setup.

6.3.3 Installation Instructions for Microsoft Windows:

To install the software, you often require administrator rights. Ask your system administrator for help if you do not have these rights on your local computer. You should shut down the programme once it has finished installing and is running in order to log back in as an ordinary user for security reasons.

You can skip this step if you already have a recent installation DVD. But, there are some other items available for free in the download area as well. Please take into account the licence conditions of each specific product.

Run the installer by double-clicking setup.exe in the installation package's root folder if you have downloaded an installation package or if the DVD installation does not begin automatically when you insert it into your DVD drive. The screen that follows will appear:

The following step will be to install several modules needed by the CST Studio Suite programme, depending on the existing system configuration:

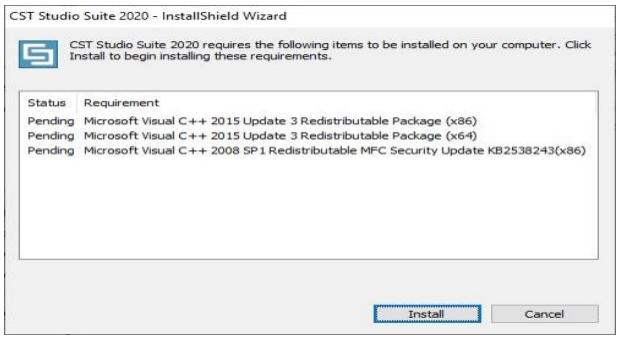

Fig.6.3.3.1 CST Studio Suite 2020- Initialisation Interface.

Certain modules, or even the entire dialogue box, may not be displayed if some or all of these prerequisites are already met. Please click Install to continue with the software installation, which will then display the screen below:

Fig.6.3.3.2 CST Studio Suite 2020- Welcome Interface.

Then, follow the directions on the screen, and as you move along, make sure to read every screen. To make sure you can access all examples that might be of interest to you, we advise adopting the *typical* setup.

Please be aware that the installation of Distributed Computing components, which can be engaged later, is now part of the usual setup.

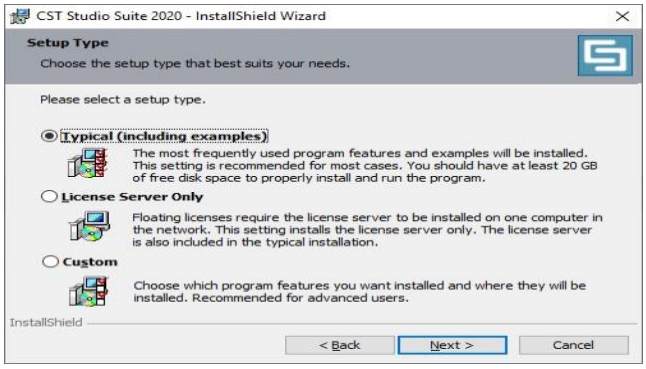

Fig.6.3.3.3 CST Studio Suite 2020- Select Setup Type Interface.

Please make sure to install the MATLAB Runtime package after selecting Next and Install. If you wish to utilise IDEM or FEST3D, you must have it:

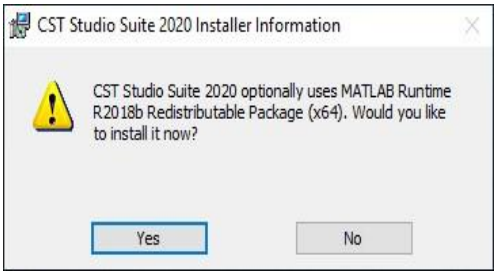

Fig.6.3.3.4 CST Studio Suite 2020- Installer Interface.

The following dialogue box occurs following installation completion:

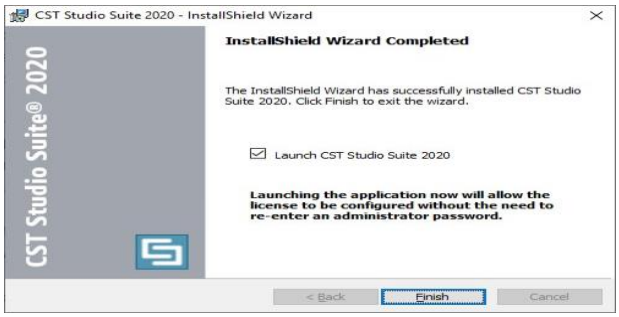

.

Fig.6.3.3.5 CST Studio Suite 2020- InstallShield Wizard Completed.

6.3.4 License Server:

Using a floating (or network) licence requires the operation of a licencing server on one computer in your network that is accessible by all other machines running CST Studio Suite software. The licencing server and the other modules always communicate via TCP/IP. If a firewall is being utilised, make sure the connections can be established.

A standalone installation of a licence server is only required if you wish to utilise the licence server on a machine without the CST Studio Suite Program Files component installed on it. The licence server is always included in the installation of common software. Skip the installation stage and continue with the licence server setup if the CST Studio Suite simulation software is already installed on the licencing server.

6.3.4.1 License Server Installation:

It is simple to set up the licence server on a certain computer. Run the installation programme by following the instructions on the preceding pages. When prompted, choose License Server as the installation type.

6.3.4.2 License Server Configuration:

You must configure the licence once the licence server has been installed. The Windows Start menu's CST Studio Suite 2020 folder contains links to the CST Studio Suite components. CST License Manager is a file in this folder. To open the License Server control panel, select this entry:

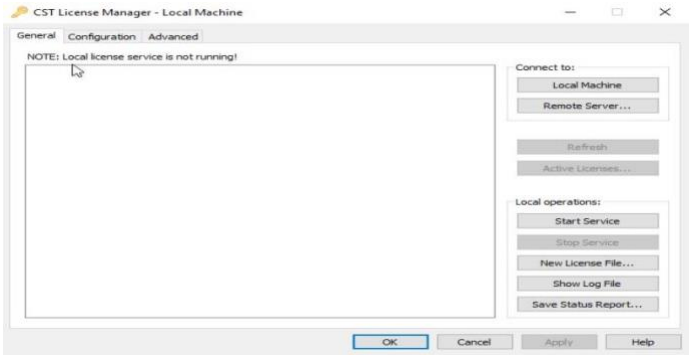

Fig.6.3.4.2 CST License Manager.

Click the New License File button to continue. The licence file, which you ought to have received by email, will need to be located later on when you are invited to do so. The new licence file will immediately be copied to the appropriate directory once it has been properly selected. The licence server must then be started by clicking the Start Service button. A list of the current licences that are available will be shown in the Licenses available on local server list.

If the licence has been set up properly, the dialogue box should resemble the example in the following image:

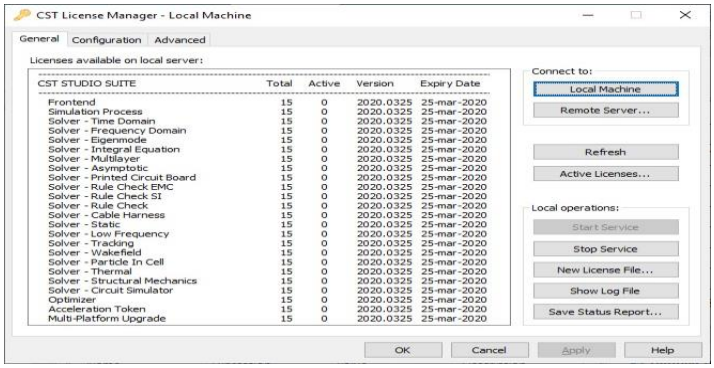

Fig.6.3.4.2.1 CST License Manager- Local Machine.

6.3.5 Starting CST Studio Suite:

A dialogue box will show up when you launch CST Studio Suite for the first time or once the licence has run out:

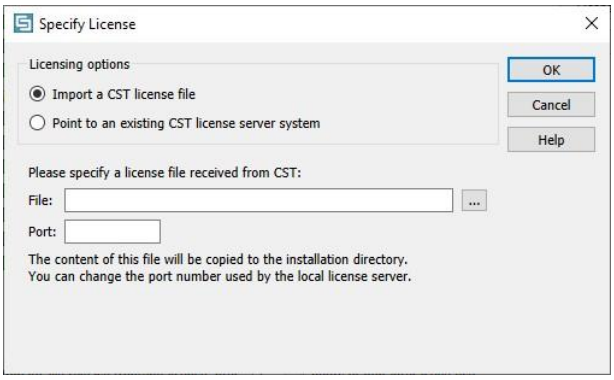

Fig.6.3.5 CST Studio Suite 2020-Specify License

Depending on whether you're going to utilise a node locked or floating licence, the next stages will be slightly different.

6.4 Node Locked License:

To install a node locked licence, choose the Import a CST licence file option in the Specify License dialogue box as shown above. By selecting the button that you should have received via email, you can then choose where the licencing file is located. The CST Studio Suite should begin when you click OK, and the licence file will be transferred automatically to the proper area.

6.5 Floating License:

A licence server must be running on one of the machines in your network in order to support floating licences. By carefully following the directions in the License Server section above, we'll presume that you've already appropriately configured your licence server. If not, install the licence server right away before moving on to the further stages.

Choose the Point to an Existing CST License Server System option for floating licences. The following dialogue box will then show up:

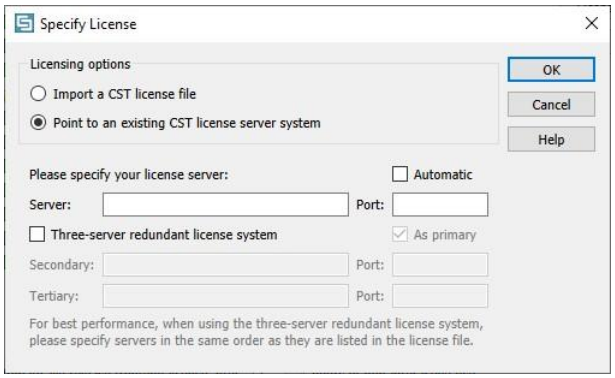

Fig.6.5 CST Studio Suite 2020- Select Floating License.

The name of your licence server must be entered in the Server box as the only setting. You can, at your discretion, enter the TCP/IP port number for the licence server in the Port field. The port will automatically be detected by default, so you can typically leave the default setting in place. Once this setting has been saved, pressing OK will launch CST Studio Suite.

6.6 User Interface:

Remember to log in as standard user rather than maintaining administrator credentials after the software has been successfully installed for security reasons.

Choose the CST Studio Suite entry from the CST Studio Suite 2020 folder in the Windows Start menu to launch the programme. The primary window of the CST Studio Suite user interface will appear to you:

Fig.6.6 CST Studio Suite 2020- User Interface

This is the application's default display when no projects are open. Selecting the File tab will enable it at any time.

You have easy access to common file-related tools like Open, Save, and Print on the left pane. Four additional pages are offered in addition to those common controls:

- **Project**: A brief summary of the current project is provided on the Project page, which also provides access to project-related functions like Archive Asor easy access to the project folder in Windows Explorer. Please be aware that only if a project is loaded can you view this page.
- **New and Recent**: The primary location to begin a new project or rapidly load one of the most recent projects is the New and Recent page.
- **Component Library**: You can organise and distribute your reusable projects with your coworkers on the Component Library page. Please refer to the online help system for more details on the Component Library.
- **Help**: You may access your support account, start the online assistance, and acquire copyright and version details all from the Help page.

6.7 License Management:

By selecting File License the License Management dialogue box will be displayed as:

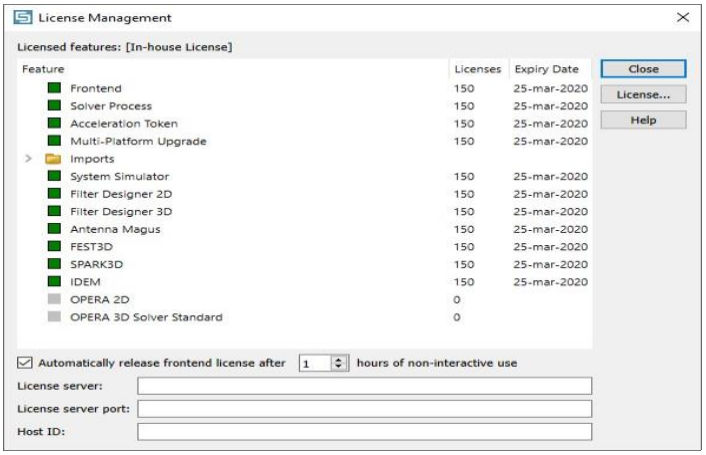

Fig.6.7 CST Studio Suite 2020-License Management.

A list of all possibly accessible features, the quantity of licences, and the dates on which each licence expires are displayed in the tree view. A tool tip with further details about each feature is displayed when the mouse is moved over one of the features.

The Host ID and presently used License server and port are displayed in additional text fields in the dialogue box.

If your licence is node locked, you can still update it by clicking the License button. We advise using the Licensing Server control panel if you are using a floating licence, as detailed in the installation instructions in Chapter 2.

6.8 Automatic Software Updates:

You can maintain your CST Studio Suite installation up to date with the aid of the automatic software update system.

The system is set up by default so that it regularly checks the internet for fresh updates. Changing this is possible by selecting File: Options

- Automatic Updates:

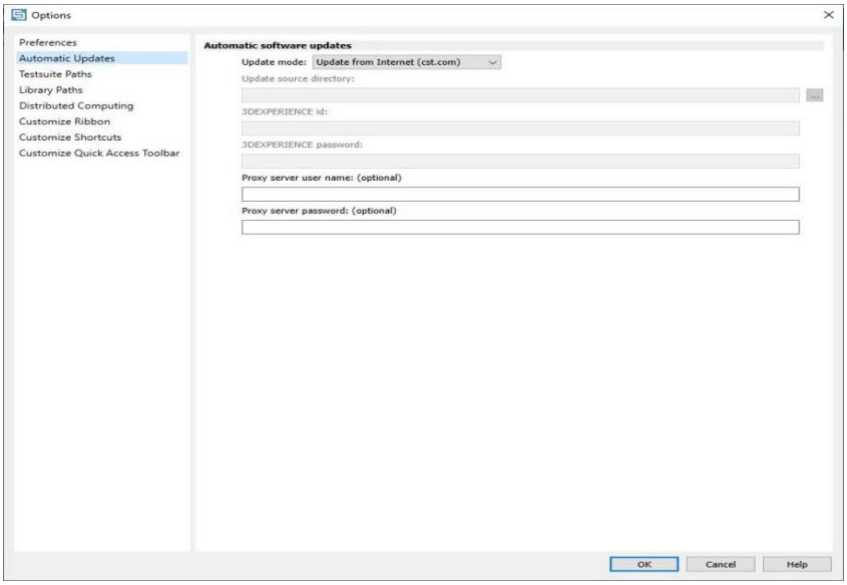

Fig.6.8 CST Studio Suite 2020- Automatic Software Update Interface.

Here, you can optionally provide proxy server information as well as the update mode (Update from Internet, Update from Local Directory, or No Automatic Updates). If you need to give authentication information when initiating an internet connection, the latter may be required.

To keep current with the most recent software changes, we strongly advise using the automated software updates. For further details about the software update mechanism, kindly consult the online help system.

6.9 Version Information:

The technical support staff may occasionally inquire as to the software version you are using. By selecting File:Help: you can quickly discover this information.

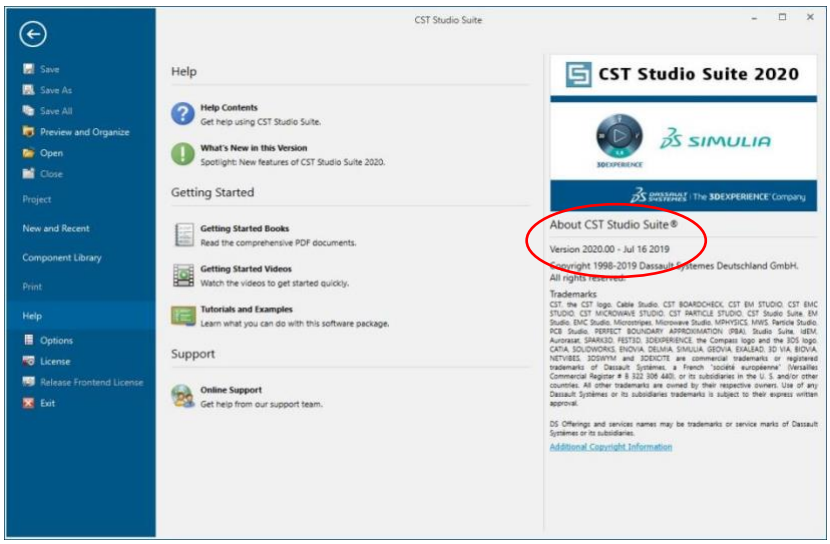

Fig.6.9 CST Studio Suite 2020-Version Information.

6.10 Opening a Project:

Employ the File: To open a current project, use the Open command:

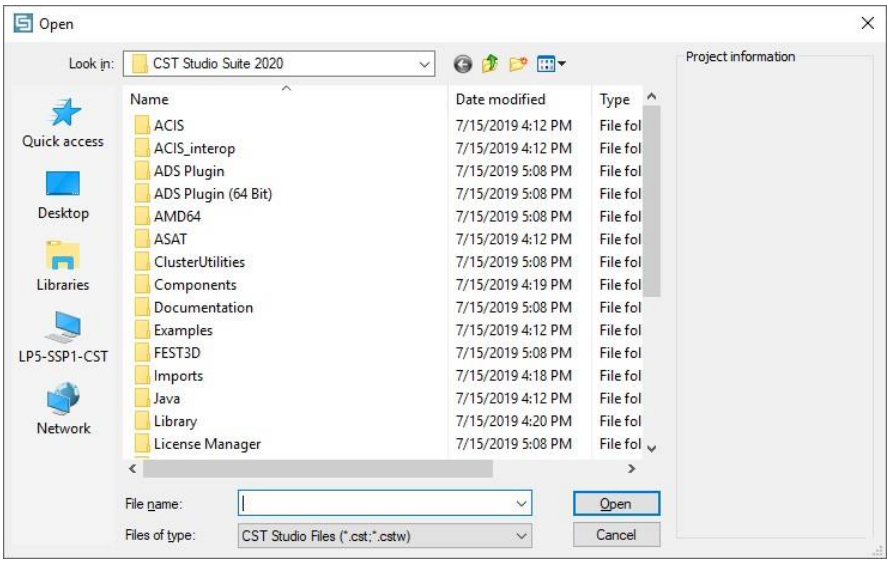

Fig.6.10. CST Studio Suite 2020-Opening a project.

You can choose a project file with the.cst extension from this list.

Simply turn on File: New and Recent, choose the project from the list of recently used projects, and click Open to access it.

6.11 Creating a New Project:

By selecting the New Template button on the New and Recent tab, a new project can be created. By pressing this, the template wizard will launch, leading you through a series of questions to define the application domain for your new project.

This guarantees that the correct module will launch automatically. Also, every project configuration is configured properly for the specific kind of device you want to examine. Moreover, a project template of these parameters is kept for future usage. To establish a new project of the same type, simply select this template from the list of project templates.

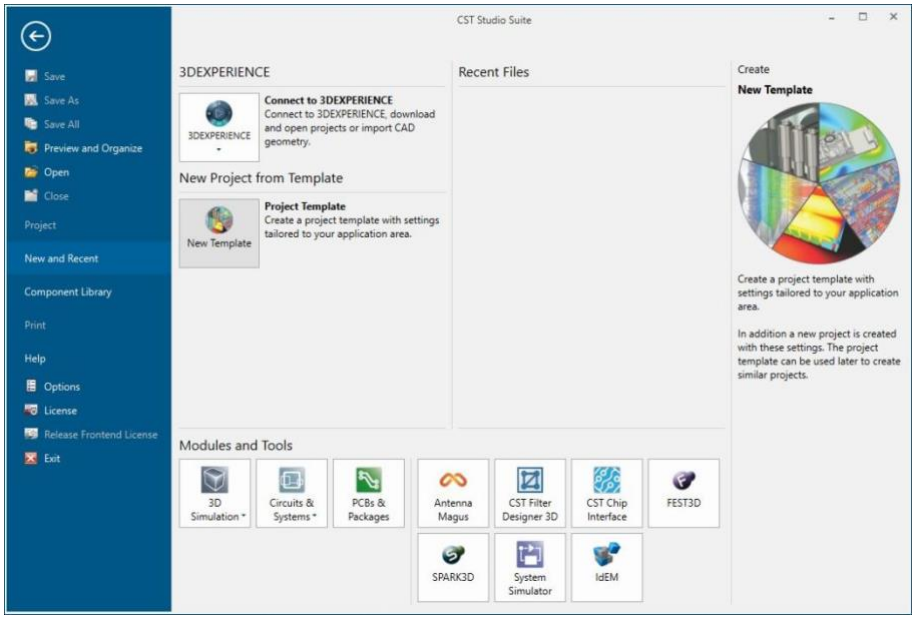

Fig.6.11 CST Studio Suite 2020- Creating a Project.

You can make a new project using the buttons in the Modules and Tools section in addition to the Template Wizard. Quick access to other applications is provided by the Tools buttons.

If you have the **3D** Experience platform installed on your computer, the button Connect to **3D** Experience is accessible. In this situation, it is simple to import CAD geometry or open projects from **3D** Experience.

We wish to start a new project right now. To launch the template wizard, click File: New and Recent New Template. In this paper, we merely outline the typical actions required while utilising this wizard to create projects. For more information, please see the other CST Studio Suite papers.

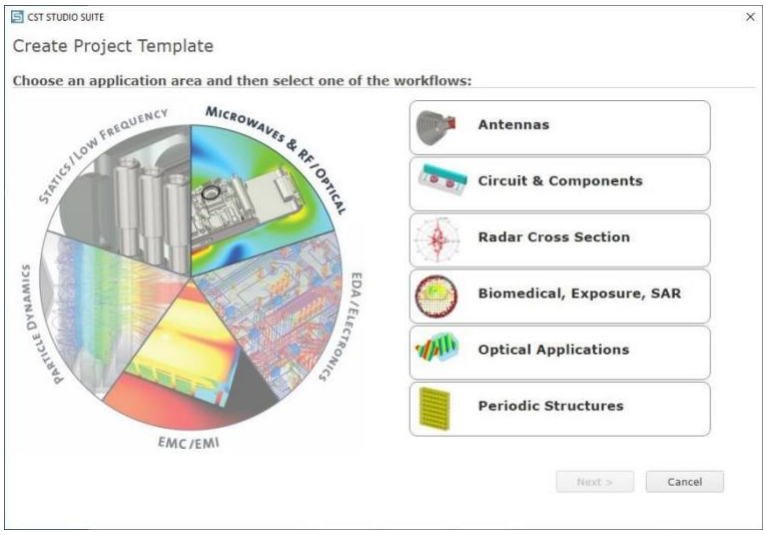

Fig.6.11.1 CST Studio Suite 2020-Project Template

We don't need any unique project settings for this introduction, so simply choose MW & RF & OPTICAL and Antennas, then repeatedly press the Next button without making any changes. On the summary page, which follows the project definition, you can confirm your selections. Change the project template's name here if necessary:

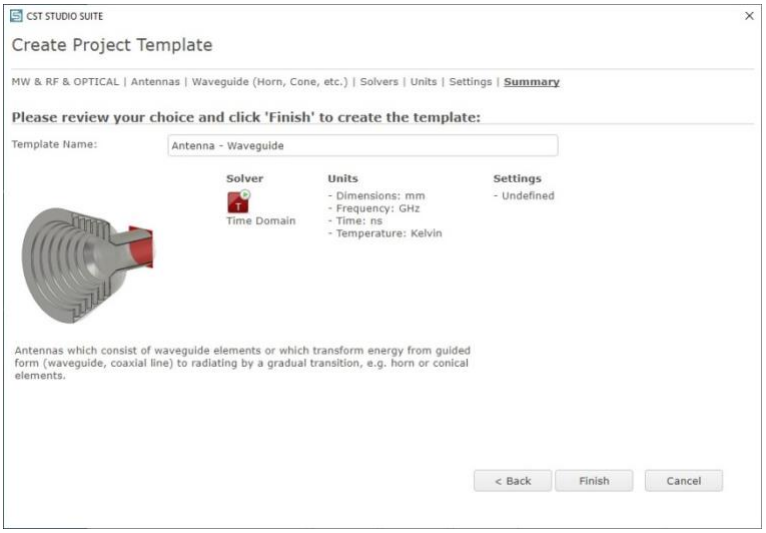

Fig.6.11.2 CST Studio Suite 2020-Creating Project Template Name.

Lastly, click Complete to launch the relevant module. This is the high frequency module CST Microwave Studio in this instance.

- Offers a range of options but does not immediately cause a response.
- The Split button combines the features of the other two kinds. When you click on the bottom of the button, a menu appears. When the upper portion is used, the control's default action is carried out.

For immediate access to these values, click on the text. Also, you can change how you use the mouse to control the display. This paper goes on to discuss the various mouse modes.

CHAPTER 7

POLARIZATION

7.1 Polarization:

1. Polarization is the phenomenon of electromagnetic radiations that explains this same link seen between orientation as well as the size of such pulsating electric field.

2. Polarizing action but rather condition of being or becoming polarized, including such altering radiation as well as particularly light whereby the oscillations or fluctuations of the wave take along a defined configuration.

3. Polarized light waves constitute light waves that really only move in what seems like a solitary plane.

7.2 Types of polarization:

There are three types of polarization, such as:

- Linear polarization.
- Circular polarization.
- Elliptical polarization.

7.2.1 Linear polarization:

In electrodynamics, the restriction of the electric field vector or magnetic field vector to a certain plane along the propagation path is known as linear polarization or plane polarization of electromagnetic radiation. Augustin-Jean Fresnel first used the word "linear polarization" (French: polarizationrectiligne) in 1822. For more information, see polarization and plane of polarization.

The direction of the electric field vector determines the orientation of an electromagnetic wave that is linearly polarized. For instance, radiation is said to be vertically polarized if the electric field vector is vertical (moving up and down as the wave travels).

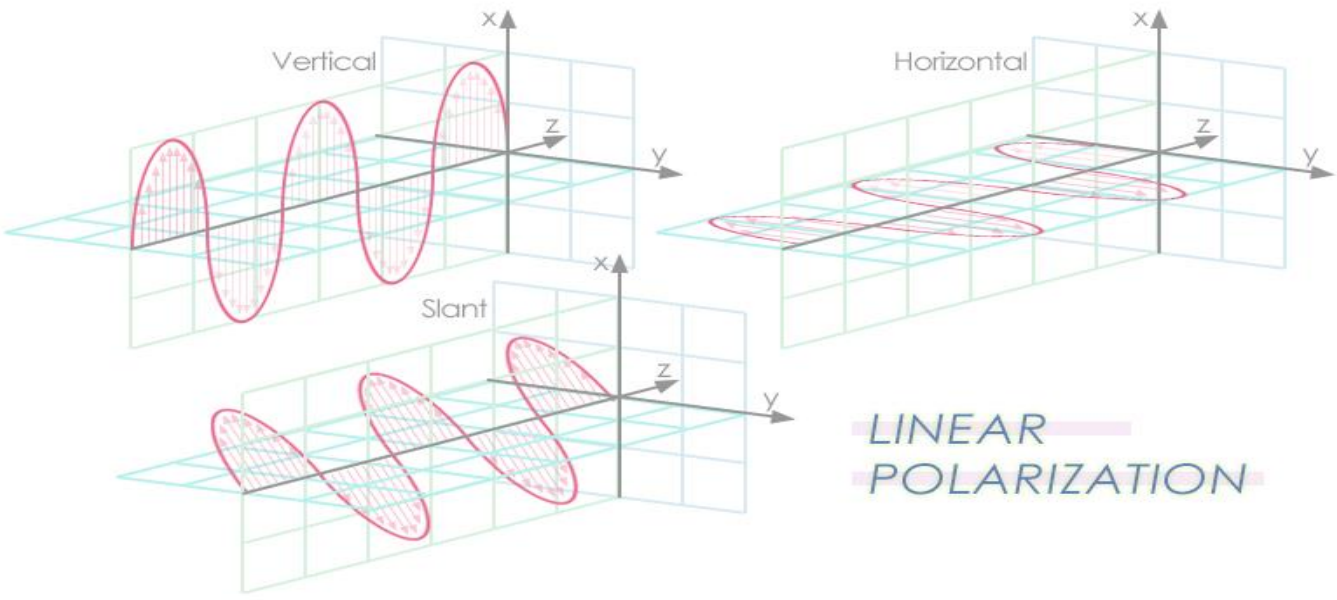

Fig.7.2.1 Linear Polarization

The most prevalent polarization in antennas is linear polarization. The electric field vector in a linear polarization antenna, as previously mentioned, moves down a line. In such a linearly polarized antenna, the electric field has just one component. If there are two components, then there will either be a 0° or 180° phase difference between them. The propagation direction is totally covered by the single plane in which the linear polarization antenna radiates.

Three categories of linear polarization antennas are distinguished:

7.2.1.1 Vertically Polarized Antenna:

A linear polarization antenna having an electric field that is oriented perpendicular to the earth's surface is said to be vertically polarized. It is recognised by a low angle of radiation close to the planet's surface as a consequence. An antenna with vertical polarization and just one vertical element may disperse the electromagnetic impulses evenly in the horizontal plane. Examples of vertically polarized antennas are whip antennas seen in automobiles and AM radio broadcasting tower antennas.

7.2.1.2 Horizontally Polarized Antenna:

Electromagnetic signals with a horizontal polarization are transmitted using linear polarization antennas. The electric field of a horizontal polarization antenna is perpendicular to the earth's surface. Television is one application of horizontal polarization antennas in communication systems.

7.2.1.3 Slant Polarized Antenna:

A slant polarized antenna is a linear polarization device that emits radiation with alternating vertical and horizontal polarization. Signals may be transmitted using slant polarized antennas utilising either vertical or horizontal polarization antennas. Radiation angles of either +45° or -45° are generally measured from the reference plane for slant polarized antennas. The polarization of the antenna may have a significant impact on both the performance of the antenna and the overall performance of a communication system. A linear polarization antenna is the ideal antenna for general radio, mobile, and short-range wireless communication systems.

7.2.2 Circular Polarization:

An electromagnetic wave is said to be circularly polarized in electrodynamics if its electromagnetic field spins continuously at each point in a plane perpendicular to the wave's direction while maintaining a constant amplitude.

The intensity and direction of an electric field are determined by the electric field vector in electrodynamics. The following animation demonstrates how, in the case of a circularly polarized wave, the phase of the light as it travels through time and space is connected to the tip of the electric field vector. The point on the helix that is parallel to the direction of propagation is indicated by the wave's electric field vector at any given time. The two possible rotations for a circularly polarized wave are right-handed circular polarization (RHCP), in which the electric field vector rotates in a right-hand sense with respect to the direction of propagation, and left-handed circular polarization (LHCP), in which the vector rotates in a left-hand sense.

A limiting example of elliptical polarization is circular polarization. The second unique instance is the simpler linear polarization. Augustin-Jean Fresnel created all three titles in a memoir that was read to the French Academy of Sciences on December 9, 1822. In 1821, Fresnel first identified the phenomenon of circular polarization but did not name it.

When light behaves as a two-dimensional transverse wave, the phenomenon of polarization results.

When the two orthogonal electric field component vectors are exactly 90°, or one-quarter wavelength, out of phase with one another and have equal magnitudes, circular polarization occurs.

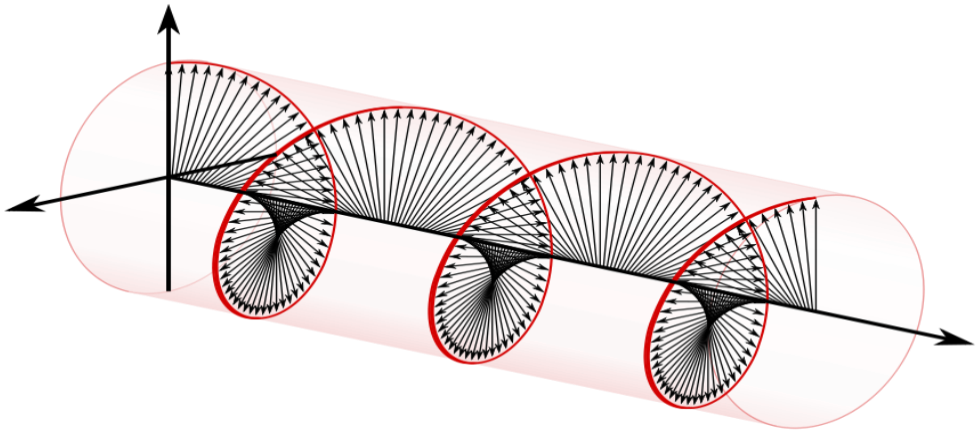

Fig.7.2.2 Circular Polarization

7.2.2.1 Right-Handed Circular Polarization:

The antenna, radio frequency (RF) section, filtering, and intermediate frequency components are located on the front of a GPS receiver. The antenna collects the satellite signals and converts the incoming electromagnetic waves into electric currents that the RF component of the receiver can comprehend. There are many different GPS antenna configurations that may be used, however antenna efficiency is essential due to the low power density of the satellite signal, particularly after it has passed through the atmosphere. GPS antennas must thus have a high gain or sensitivity. They may be programmed to collect L1 signals exclusively, L1 signals and L2 signals, or all signals, including L5. Similar to the GPS signals that are broadcast from satellites, they must always be Right Hand Circular Polarized (RHCP).

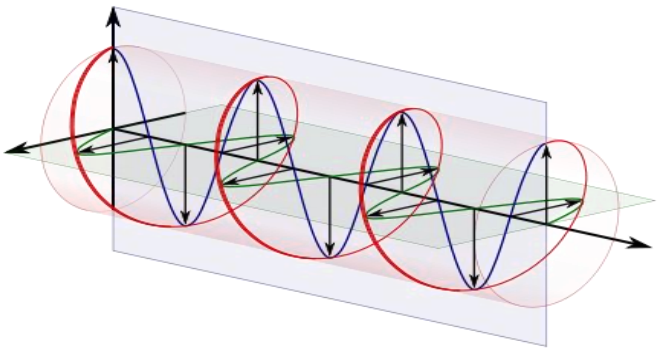

Fig.7.2.2.1 Right hand circular polarization

Polarized waves may oscillate in a number of different directions. Although the direction of the electrical field vectors in the GPS signal rotates, their amplitude remains constant, giving the wave's electrical field vector the appearance of a helix as it moves. In other

words, circularly polarized waves are those in which the angle of the electric vector rotates around a fictitious line travelling in the direction of the wave. Either the left or the right may be rotated. The GPS signal is made up of right-handed circularly polarized (RHCP) waves. This is an example of one method. Use your right hand to give the thumbs-up signal. Now, instead of pointing your thumb upward, do so in the GPS signal's direction. Your fingers are curved such that you can see the axis of rotation of the field.

7.2.2.2 Left-Handed Circular Polarization:

On the right, the electric field vectors of a circularly polarized electromagnetic wave are shown. The composite vector of the individual electric field vectors and its magnitude and phase angle remain constant. The fact that this is a plane wave means that each vector represents the magnitude and direction of the electric field for an entire plane that is parallel to the optical axis. These vectors explicitly demonstrate that for this circularly polarized plane wave, the electric field rotates consistently in direction and maintains a constant intensity from plane to plane. Please see these two images from the plane wave page to better grasp this dynamic. This light is believed to be circularly polarized in the right hand, clockwise, if it is detected by the receiver. Given that this is an electromagnetic wave, each electric field vector has a corresponding magnetic field vector that is at a right angle to it and has a magnitude proportional to it. Not visible is the magnetic field vector. The magnetic field vectors would so create a second helix if they were shown.

The electromagnetic wave shall simply be referred to as light in this section because circular polarization is frequently encountered in the realm of optics.

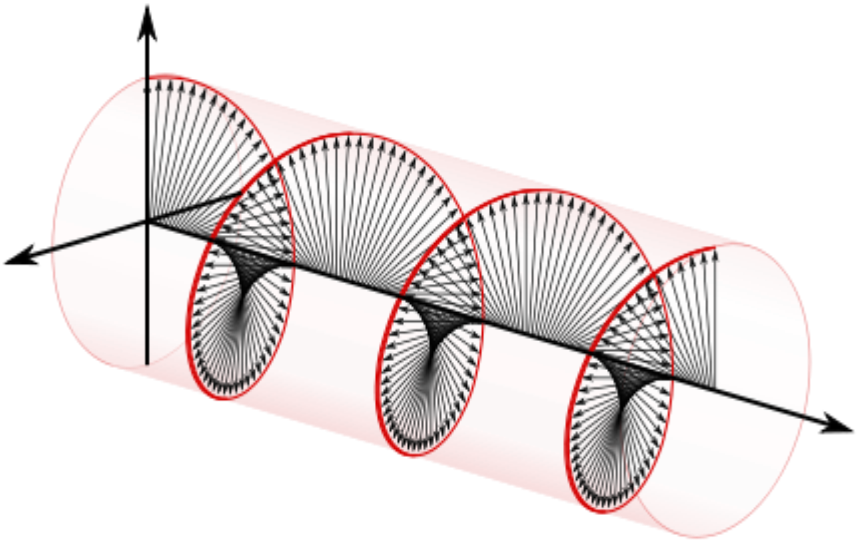

Fig.7.2.2.2 Left-handed circular polarization

To understand the nature of circular polarization and its connection to other polarizations, it is usual to see the electric field as being divided into two components that are perpendicular to one another. The vertical component and its corresponding plane are depicted in blue, while the horizontal component and corresponding plane are shown in green. Remember that the

horizontal and vertical components are 90° out of phase, with the horizontal component travelling to the right (relative to the direction of motion). According to this quadrature phase connection, which also gives birth to the helix, the places of the highest magnitude of the vertical component coincide with the points of zero magnitude of the horizontal component, and vice versa. This alignment results in vectors that completely match the maxima of the vertical and horizontal components and correspond to the helix.

To see how this quadrature phase shift relates to an electric field rotating while maintaining a constant magnitude, consider a dot travelling in a circle anticlockwise. Consider how the dot's horizontal and vertical distances from the centre of the circle change over time sinusoidally and are off by one-quarter of a cycle. The displacements are said to be out of phase by one quarter of a cycle because the horizontal maximum displacement (towards the left) is obtained one quarter of a cycle before the vertical maximum displacement. Think of the circle's centre travelling along the axis from the front to the back, using the image as a reference once again. With the vertical displacement guiding the displacement towards our viewing left, the rotating dot will form a helix. Like the horizontal and vertical displacements of the spinning dot, the amplitude of the horizontal and vertical components of the electric field are out of phase by a quarter of a wavelength.

7.2.3 Elliptical Polarization:

Elliptical polarization, a generalization of circular polarization, is the third prevalent kind of polarization. It happens when the two linear, perpendicular components of the electric field are out of phase by 90 degrees and have different magnitudes. An elliptically polarized antenna may be polarized in either the right or left hand, similar to circular polarization. elliptical and circular polarizations.

Having stated that, once a radio wave is launched by an antenna, its properties are constantly changing. Hence, as the wave reaches the receiving antenna, it often experiences fading, reflections, multipath interference, phase shifts, and many other effects that are unique to the operating environment (urban or rural, for example), which have an impact on the received signal intensity. The issues for any kind of system start here since these elements may greatly reduce the signal's quality and intensity.

The following information will focus on the areas between about 600 MHz to 3700 MHz where cellular and other services are presently offered. As attenuation and changes in signal properties are negligible at these frequencies (see Figure 3), propagation is best achieved across an unobstructed visual line-of-sight (LOS) route between the transmitter and receiver. LOS is the perfect situation for a wireless transmission since the propagation challenge is solely posed by the characteristics of the operating frequency and the weather or atmospheric conditions. As a consequence, the transmission line may be extended and the signal intensity increased, increasing throughput.

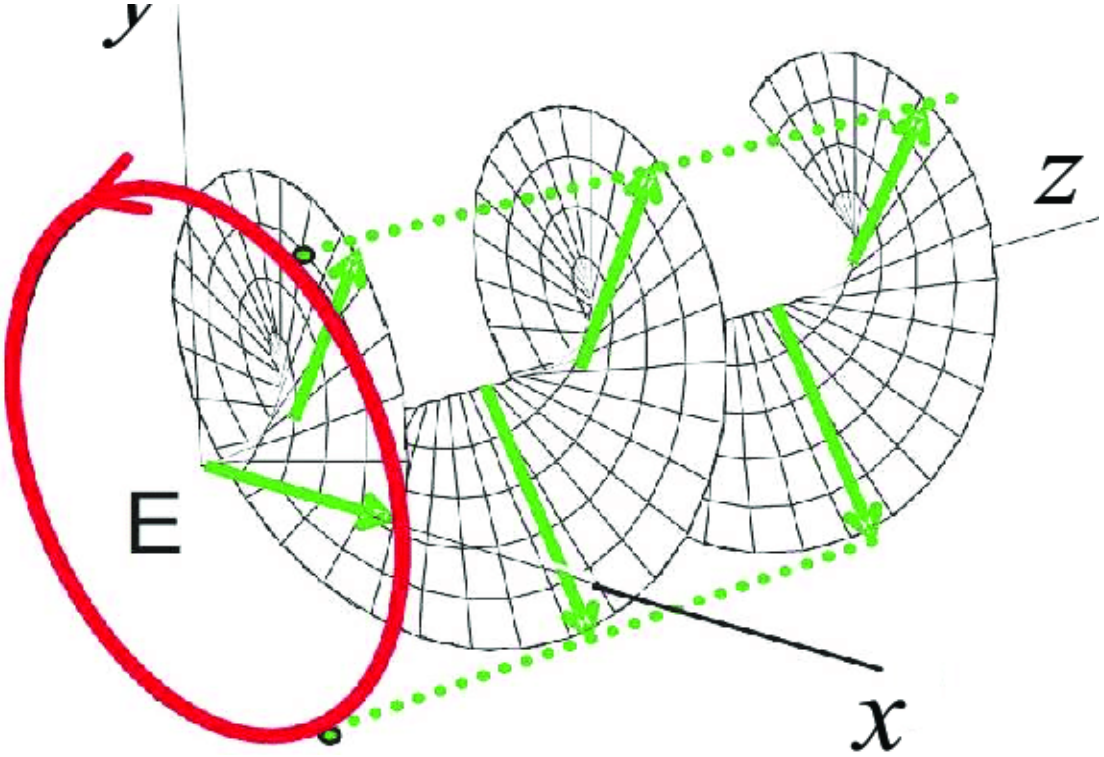

Fig.7.2.3 Elliptical Polarization

Ellipsoidal polarisation in electrodynamics is the polarisation of electromagnetic radiation when the electric field vector's tip defines an ellipse in any given plane crossing and perpendicular to the propagation direction. A wave that is elliptically polarised may be split into two waves that are linearly polarised and have right angles between their polarisation planes. Ellipsobatically polarised waves demonstrate chirality because the electric field may spin either clockwise or anticlockwise as it moves through space.

CHAPTER 8

STRUCTURE DESIGN

8.1 PROPOSED STRUCTURE:

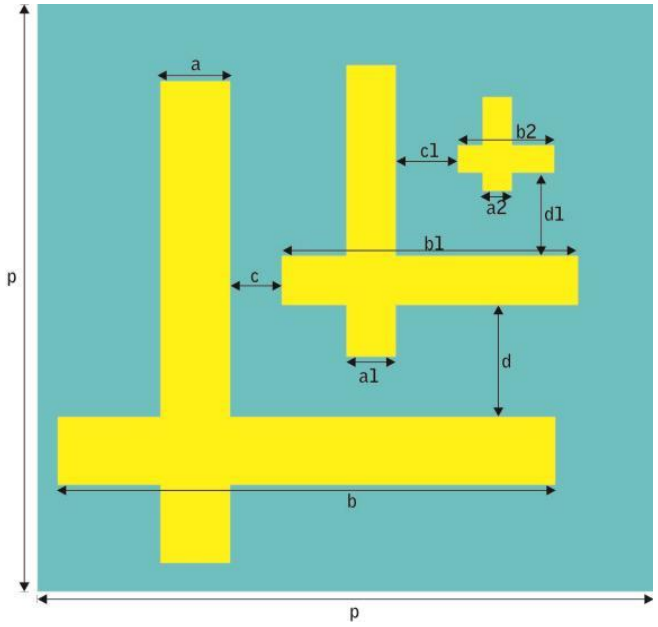

Fig.8.1.1 A polarization converter unit's front view schematic diagram

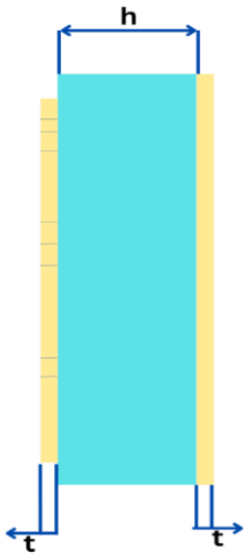

Fig.8.1.2 Diagrammatic representation of the side view of a polarization converter unit.

8.2 PARAMETRIC OPTIMIZATION:

The metasurface's unit cell is depicted in Fig.8.1.1 Polyimide, which has a relative dielectric constant of 3.5, a length of 120 micrometres and a thickness of 50 micrometres, is the dielectric material we've chosen since it is micron-level flexible. With a conductivity of 6.30 x 107 S/m and a thickness of 0.3 micrometre, silver makes up the top and bottom layers. The parameters of the three cross structures are:

p= 140 µm, a = 14 µm, b = 100 µm, a1 = 10 µm, b1 = 60 µm, a2 = 6 µm, b2 = 20 µm,

c = 11 µm, d = 18 µm, c1 = 14 µm, d1 = 12 µm, h= 50 µm, t=0.3 µm.

Table 2

Design Specifications:

Parameters	Dimension	Materials Used
Length of the Substrate(p)	140 µm	Polyimide
Length of the Ground plane(p)	140 µm	Silver
Thickness of Substrate(h)	50 µm	Polyimide
Thickness of Ground plane and solids(t)	0.3 µm	Silver
Length of solid1(b)	100 µm	Silver
Length of solid2(b1)	60 µm	Silver
Length of solid3(b2)	20 µm	Silver
Width of solid1(a)	14 µm	Silver
Width of solid2(a1)	10 µm	Silver
Width of solid3(a2)	6 µm	Silver
Gap between solid1 & solid2(c)	11 µm	Silver
Distance between solid1 & solid2(d)	18 µm	Silver
Gap between solid2 & solid3(c1)	14 µm	Silver
Distance between solid2 & solid3(d1)	12 µm	Silver

CHAPTER 9

RESULTS AND DISCUSSION

9.1 Results & Discussions:

9.1.1 Reflection Coefficient:

The reflection coefficient, also known as the reflection factor, is a measure of the fraction of an incident electromagnetic wave's power that is reflected back from a boundary between two materials. It is a dimensionless quantity that is often denoted by the symbol "R".

The reflection coefficient depends on the properties of the two materials at the boundary, such as their refractive indices, impedance, and absorption coefficients. It is usually defined as the ratio of the amplitude of the reflected wave to that of the incident wave:

$$R = |Er| / |Ei|$$

where |Er| is the amplitude of the reflected wave and |Ei| is the amplitude of the incident wave. The reflection coefficient can also be expressed in terms of the electric field or magnetic field vectors of the incident and reflected waves.

The reflection coefficient can take on values between 0 and 1, with 0 indicating no reflection and 1 indicating total reflection. In general, the reflection coefficient is a function of the angle of incidence and the polarization state of the incident wave. The reflection coefficient can be measured experimentally using techniques such as reflectometry, interferometry, or spectroscopy.

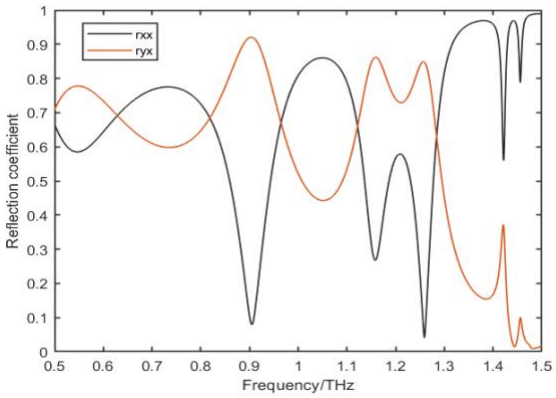

Fig.9.1.1 Reflection of the polarization converter under co- and cross-polarization Coefficient

From the above graph we can observe that the cross-polarization coefficient r_{yx} is greater than 0.85 and the co-polarization coefficient r_{xx} is less than 0.3 in the dual bands of 0.8726~0.8924 THz, 1.1075~1.1147 THz, and 1.2614~1.2731 THz.

9.1.2 Phase Plot:

A phase plot of a metasurface shows the variation of the phase of the reflected or transmitted wave as a function of the incident angle or wavelength.

In general, the phase response of a metasurface depends on the geometry and arrangement of the meta-atoms, as well as the polarization and frequency of the incident wave. By controlling the phase response, a metasurface can achieve a range of functionalities such as anomalous reflection, polarization conversion, beam steering, and wavefront shaping.

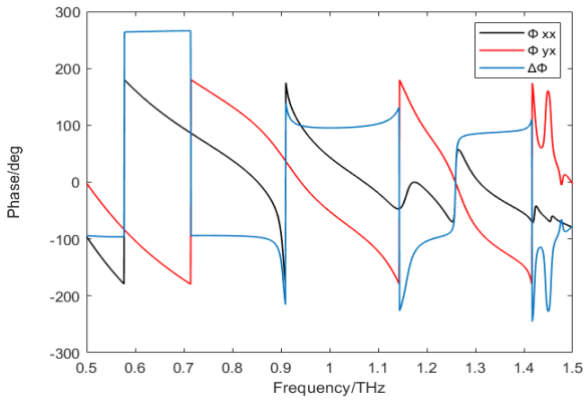

Fig.9.1.2 Reflection of the polarization converter under co- and cross-polarization in Phase

9.1.3 PCR:

Polarization conversion ratio (PCR) is a measure of the efficiency of the conversion of the polarization state of light in a medium. When light interacts with a material, the polarization state of the light can be changed due to the birefringence or anisotropy of the material. The PCR is defined as the ratio of the output power of the converted polarization state to the input power of the incident polarization state.The PCR can be expressed mathematically as:

PCR = output power of converted polarization state / input power of incident polarization state

$$PCR = \frac{|r_{yx}|^2}{|r_{yx}|^2 + |r_{xx}|^2}$$

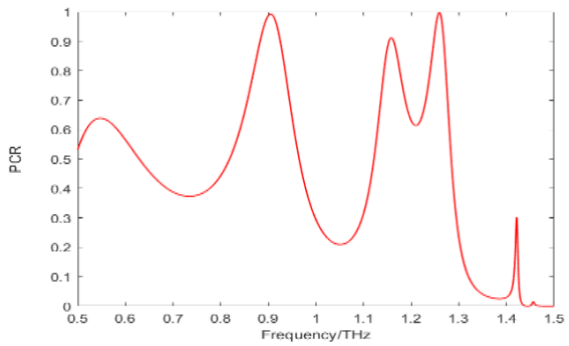

Fig.9.1.3 The reflected waves polarization conversion rate (PCR)

The above Fig demonstrates successful LCP conversion and the converter's PCR is greater than 95%, as shown in Fig9.1.3.

9.1.4 Ellipticity:

Ellipticity is a property of polarized light that describes the degree to which the polarization state deviates from being perfectly linear. Elliptically polarized light has a polarization state that can be described as an ellipse in the plane perpendicular to the direction of propagation.

The ellipticity of polarized light is characterized by the ellipticity angle, which is the angle between the major axis of the polarization ellipse and the direction of linear polarization. The ellipticity angle can take on values between 0 and 90 degrees, with 0 degrees indicating linear polarization and 90 degrees indicating circular polarization.

The degree of ellipticity is often quantified by the ellipticity ratio, which is the ratio of the minor axis of the polarization ellipse to its major axis. The ellipticity ratio can take on values between 0 and 1, with 0 indicating linear polarization and 1 indicating circular polarization.

Elliptically polarized light can be generated by various mechanisms, such as birefringent materials, wave plates, or by the interaction of light with magnetic fields or chiral materials. Applications of elliptically polarized light include polarization-sensitive imaging, optical communications, and spectroscopy.

The Stokes equations in optics can be used to obtain the ellipticity equations of the reflective converter.

$S_0 = r^2_{xx} + r^2_{yx}$

$S_1 = r^2_{xx} - r^2_{yx}$

$S_2 = 2r_{xx}\, r_{yx} \cos \delta$

$S_3 = 2r_{xx}\, r_{yx} \sin \delta$

Where $\delta = \Phi_x - \Phi_y$ is the phase difference between r_{xx} and $r_{yx,}$ whereby the ellipticity formulas can be derived:

$Ellipticity = S_3 / S_0$

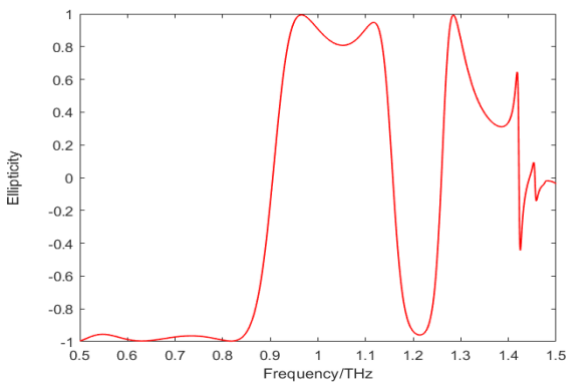

Fig.9.1.4 The reflected wave's ellipticity.

From the above graph we can observe that the dual bands of 0.516~0.862 THz, 0.947~0.986 THz, and 1.9861.203 THz, respectively, the co- and cross-polarization coefficients have comparable values ($r_{xx} \approx r_{yx}$) and a phase difference ($\Delta\Phi$) of $\pm 90^{\circ} \pm 10^{\circ}$ or $\pm 270^{\circ} \pm 10$. The converter's ellipticity can be computed, as shown in Fig.9.1.4. The ellipticity can be demonstrated to be close to ±1, with "+" and "-" standing for RHCP and LHCP, respectively, and "+" and "-" designating the bands where LTCP conversion has been achieved.

9.2 Performance review:

The coefficient and phase values for the converter's reflection qualities under an x-polarization wave's illumination are shown in Fig.9.1.1 The cross-polarization coefficient r_{yx} is greater than 0.85 and the co-polarization coefficient r_{xx} is less than 0.3 in the dual bands of 0.8726~0.8924 THz, 1.1075~1.1147 THz, and 1.2614~1.2731 THz. This demonstrates successful LCP conversion and the converter's PCR is greater than 95%, as shown in Fig9.1.3. Also, for the dual bands of 0.516~0.862 THz, 0.947~0.986 THz, and 1.9861.203 THz, respectively, the co- and cross-polarization coefficients have comparable values ($r_{xx} \approx r_{yx}$) and a phase difference ($\Delta\Phi$) of $\pm 90^{\circ} \pm 10^{\circ}$ or $\pm 270^{\circ} \pm 10$. The converter's ellipticity can be computed, as shown in Fig.9.1.4 . The ellipticity can be demonstrated to be close to ±1, with "+" and "-" standing for RHCP and LHCP, respectively, and "+" and "-" designating the bands where LTCP conversion has been achieved.

CONCLUSION AND FUTURE WORK

The dual-functional terahertz metasurface polarisation converter clearly outperforms other designs in a variety of ways when compared to the most recent metasurface polarisation converter, as shown in Table 1. In terms of operational effectiveness, polarisation conversion ratio (PCR), maximum linear-to-circular polarisation (LTCP) conversion bandwidth (FBW), and ellipticity of reflected waves, it performs better than rivals. Moreover, a wide range of angular stability is shown. Moreover, the suggested converter incorporates an easy-to-fabricate top metal pattern layer. Last but not least, this work introduces a novel design approach that has not previously been reported, achieving multiband and multifunction polarisation conversion by merging variable pattern structures and structures of various sizes in the u and v directions. The knowledge offered by this design plan may be very useful in developing future metasurface polarisation converter designs.

Finally, a proposal for a multi-band, dual-functional metasurface terahertz polarisation converter built on three asymmetric Jerusalem cross structures. The recommended converter displays LCP behaviour in a triple frequency range between 0.8726~0.8924 THz, 1.1075~1.1147THz, and 1.2614~1.2731THz. The PCR of the converter is greater than 95% in these two operational bands, and the ellipticity of the reflected wave is nearly zero. Furthermore, at triple bands of 0.516~0.862 THz, 0.947~0.986 THz, and 1.986~1.203 THz, the suggested converter exhibits LTCP converter behaviour. Within these three operational bands, the reflected wave's ellipticity gets closer to 1. Surface current and the theory of multiple interference are used to examine the physical mechanism of polarisation conversion. The suggested converter's function, PCR, and ellipticity are all significantly superior than those of the earlier polarisation converters. Also, the converter's straightforward top metal pattern makes it manifest for a variety of applications in addition to making it simple to build. Future designs of metasurface polarisation converters can benefit from some reference experience provided by this technology. The terahertz polarisation converter that is being proposed can be effectively employed in terahertz communication, imaging, and sensing.

REFERENCES

[1] Q. Wang, L. Xie, Y. Ying, Overview of imaging methods based on terahertz time-domain spectroscopy, Appl. Spectrosc. Rev. 57 (3) (2022) 249–264.

[2] I. Malhotra, K.R. Jha, G. Singh, Terahertz antenna technology for imaging applications: A technical review, Int. J. Microw. Wirel. Technol. 10 (3) (2018) 271–290.

[3] Y. Zhang, C. Wang, B. Huai, et al., Continuous-wave THz imaging for biomedical

samples, Appl. Sci. 11 (1) (2020) 71.

[4] J. Hao, Q. Ren, Z. An, et al., Optical metamaterial for polarization control, Phys.

Rev. A 80 (2) (2009) 023807.

[5] L.H. Nicholls, F.J. Rodríguez-Fortuño, M.E. Nasir, et al., Ultrafast synthesis and switching of light polarization in nonlinear anisotropic metamaterials, Nat. Photonics 11 (10) (2017) 628–633.

[6] S. Zhang, Z. Li, F. Xing, Review of polarization optical devices based on graphene

materials, Int. J. Mol. Sci. 21 (5) (2020) 1608.

[7] C.L. Holloway, E.F. Kuester, J.A. Gordon, et al., An overview of the theory and

applications of metasurfaces: The two-dimensional equivalents of metamaterials, IEEE Antennas Propag. Mag. 54 (2) (2012) 10–35.

[8] Q. He, S. Sun, S. Xiao, et al., High-efficiency metasurfaces: principles, realizations, and applications, Adv. Opt. Mater. 6 (19) (2018) 1800415.

[9] G. Moon, J. Choi, C. Lee, et al., Machine learning-based design of meta-plasmonic

biosensors with negative index metamaterials, Biosens. Bioelectron. 164 (2020) 112335.

[10] M.R. Hashemi, S. Cakmakyapan, M. Jarrahi, Reconfigurable metamaterials for

terahertz wave manipulation, Rep. Progr. Phys. 80 (9) (2017) 094501.

[11] H.T. Chen, A.J. Taylor, N. Yu, A review of metasurfaces: physics and applications,

Rep. Progr. Phys. 79 (7) (2016) 076401.

[12] X. Wen, J. Zheng, Broadband THz reflective polarization rotator by multiple

plasmon resonances, Opt. Express 22 (23) (2014) 28292–28300.

[13] W. Pan, D. Shen, Y. Yan, Design of broadband polarization converter for terahertz

waves, Optoelectron. Lett. 14 (6) (2018) 434–437.

[14] T.N. Cao, M.T. Nguyen, N.H. Nguyen, et al., Numerical design of a high efficiency

and ultra-broadband terahertz cross-polarization converter, Mater. Res. Express

8 (6) (2021) 065801.

[15] D. Wang, Y. Gu, Y. Gong, et al., An ultrathin terahertz quarter-wave plate using

planar babinet-inverted metasurface, Opt. Express 23 (9) (2015) 11114–11122.

[16] Y. Jiang, L. Wang, J. Wang, et al., Ultra-wideband high-efficiency reflective linear-to-circular polarization converter based on metasurface at terahertz frequencies, Opt. Express 25 (22) (2017) 27616–27623.

[17] W. Pan, X. Ren, Q. Chen, A terahertz quarter wave plate based on staggered split ring resonators, Prog. Electromagn. Res. Lett. 85 (2019) 117–123.

[18] Z. Song, J. Zhang, Achieving broadband absorption and polarization conversion with a vanadium dioxide metasurface in the same terahertz frequencies, Opt. Express 28 (8) (2020) 12487–12497.

[19] Z. Li, R. Yang, J. Wang, et al., Multifunctional metasurface for broadband absorption, linear and circular polarization conversions, Opt. Mater. Express 11 (10) (2021) 3507–3519.

[20] Y. Wang, R. Yang, Y. Zhao, et al., Independently tunable bifunctional terahertz

metasurface based on double-layer graphene, Opt. Mater. 132 (2022) 112793.

[21] Y. Jiang, M. Zhang, W. Wang, et al., Reflective and transmissive crosspolarization converter for terahertz wave in a switchable metamaterial, Phys. Scr. 97 (1) (2022) 015501.

[22] Y. Zhao, R. Yang, J. Wang, et al., Dual-mode terahertz broadband polarization

conversion metasurface with integrated graphene-VO2, Opt. Commun. 510 (2022) 127895.

[23] Y. Zhao, R. Yang, Y. Wang, et al., VO2-assisted multifunctional metamaterial

for polarization conversion and asymmetric transmission, Opt. Express 30 (15) (2022) 27407–27417.

[24] J. Wang, R. Yang, Z. Li, et al., Reconfigurable multifunctional polarization converter based on asymmetric hybridized metasurfaces, Opt. Mater. 124 (2022) 111953.

[25] M.I. Khan, Z. Khalid, S.A.K. Tanoli, et al., Multiband linear and circular polarization converting anisotropic metasurface for wide incidence angles, J. Phys. D: Appl. Phys. 53 (9) (2019) 095005.

[26] Q. Zheng, C. Guo, G.A.E. Vandenbosch, et al., Dual-broadband highly efficient

reflective multi-polarisation converter based on multi-order plasmon resonant metasurface, IET Microw. Antennas Propag. 14 (9) (2020) 967–972.

[27] R. Dutta, J. Ghosh, Z. Yang, et al., Multi-band multi-functional metasurface-based

reflective polarization converter for linear and circular polarizations, IEEE Access 9 (2021) 152738-152748.

[28] F. Hao, J. Zang, Design of a butterfly shaped reflective multifunctional polarization converter, in: 2022 IEEE 5th International Conference on Electronic Information and Communication Technology, ICEICT, IEEE, 2022, pp. 523–525.

[29] J.S. Li, F.Q. Bai, Dual-band terahertz polarization converter with high-efficiency asymmetric transmission, Opt. Mater. Express 10 (8) (2020) 1853–1861.

[30] R.M.H. Bilal, M.A. Baqir, P.K. Choudhury, et al., On the specially designed fractal

metasurface-based dual-polarization converter in the THz regime, Results Phys. 19 (2020) 103358.

[31] H. Luo, X. Wang, H. Qian, Multi-functional high-efficient reflective polarization converter based on all-metal stereostructured anisotropic metamaterials at terahertz frequency, Opt. Commun. 519 (2022) 128403.

PUBLICATION DETAILS: Communicated to Journal (Plasmonics)

A MUTI-BAND POLARIZATAION CONVERTOR WITH DUAL FUNCTIONALITIES BASED ON A ASYMMETRIC CRUCIFORM SHAPED METASURFACE AT TERAHERTZ FREQUENCY

1. Mrs.B.Rama Devi (Ph.D.)
Department of ECE,
ANITS, Visakhapatnam, AP, India
ramadevi.ece@anits.edu.in

2. K.Jyothir Sai *
Department of ECE,
ANITS, Visakhapatnam, AP, India
jyothirsai.2019.ece@anits.edu.in

3. B.Keerthi
Department of ECE,
ANITS, Visakhapatnam, AP, India,
keerthi.2019.ece@anits.edu.in

4. S.Raviteja
Department of ECE,
ANITS, Visakhapatnam, AP, India,
raviteja.2019.ece@anits.edu.in

5. M.Surya Vamsi
Department of ECE,
ANITS, Visakhapatnam, AP, India,
suryavamsi.2019.ece@anits.edu.in

*Corresponding author email : **jyothirsai.2019.ece@anits.edu.in**

Abstract— In this paper, a terahertz wave polarization converter is proposed as the metasurface. Resonators in a cross form make up the unit cell. The suggested metasurface performs as a linear to cross polarization converter with a polarization conversion ratio more than 95% and ellipticity zero for the reflected wave at the frequency bands 0.8726~0.8924 THz, 1.1075~1.1147 THz, and 1.2614~1.2731 THz. It also demonstrates the traits of a linear to circular polarization converter over frequency ranges of 0.516~0.862 THz, 0.947~0.986 THz, and 1.986~1.203 THz. For these three frequency ranges, the reflected wave's ellipticity is between -1 and +1. Up to 500 degrees of oblique incidence, the suggested metasurface is angularly stable. Surface current distribution and multiple interference theory are used to investigate the fundamental mechanism of polarization conversion. The converter has potential uses in terahertz detection, assessing the absorption spectrum of complex biological samples, and satellite communication due to its straightforward structure, angular stability, and dual functionality.

Keywords— Terahertz, Metasurface, Polarization, Ellipticity.

1. INTRODUCTION:

Satellite communication and sensing are just two applications for terahertz waves, which are electromagnetic waves that exist in the electromagnetic spectrum between the microwave and infrared bands. Terahertz waves, which have frequencies between 0.1 and 10 THz, are the name given to these electromagnetic waves. Changing the polarization state of terahertz waves is the main obstacle to terahertz technology application., which is the fundamental physical characteristic of these

waves. Terahertz waves are capable of being applied in more intricate circumstances by altering the wave's polarization state.

Metasurfaces, on the other hand, are two-dimensional arrays of subwavelength features that can precisely and tightly control how electromagnetic wave characteristics are modified. Phase, amplitude, and polarization of light are frequently controlled by them. In the case of polarization manipulation, a metasurface can be designed to convert one polarization state to another, or to create a specific polarization state. This can be achieved by designing the subwavelength structures to have a specific response to each polarization state.

Metasurfaces have several advantages over metamaterials for polarization manipulation. They are easier to fabricate, since they are typically made from thin films deposited on a substrate, and they can be integrated with other optical components. They also have a lower profile, which makes them more suitable for certain applications, such as polarization conversion in integrated photonic circuits. However, metamaterials still have some advantages in terms of flexibility and tunability, and they may be more suitable for certain applications, such as sensing and imaging.

Terahertz polarization converters fall into two categories: linear to circular polarization (LTCP) converters and linear cross-polarization (LCP) converters, depending on their various functions. LTCP converters have the ability to rotate incident linearly polarized electromagnetic waves polarization direction by 90 degrees,In contrast LCP converters can change them from linear to circular polarization. The focus of current research on terahertz polarization converters is on the operational bandwidth, PCR, and ellipticity of the generated circularly polarized waves.

2. STRUCTURE DESIGN

Due to the asymmetry of the cross structure, it produces various refractive indices depending on the direction of the incident waves. As a result of the shifting refractive indices, the amplitude and phase difference meet the requirements for polarization conversion. The frequency band at which the cross structure resonates also varies with changes in cross structure size. Combining the top metal pattern layer, top dielectric layer, and bottom reflection layer results in a multiple interference cavity. Under the combined influence of surface metal resonance and various interference cavities, the effectiveness of cross- and co-polarization is evaluated.

Fig. 1 A polarisation converter unit's front

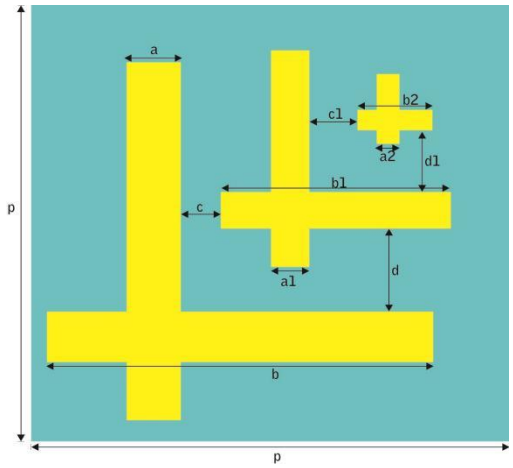

view schematic diagram

The metasurface's unit cell is depicted in Fig. 1. Polyimide, which has a relative dielectric constant of 3.5, a length of 120 micrometres and a thickness of 50 micrometres, is the dielectric material we've chosen since it is micron-level flexible. With a conductivity of 6.30 x 107 S/m and a thickness of 0.3 micrometre, silver makes up the top and

bottom layers. The parameters of the three cross structures are, p = 140 micrometers, a = 14 micrometer, b = 100 micrometer, a1 = 10 micrometer, b1 = 60 micrometer, a2 = 6 micrometer, b2 = 20 micrometer, c = 11 micrometers, d = 18 micrometers, c1 = 14 micrometers, d1 = 12 micrometers.

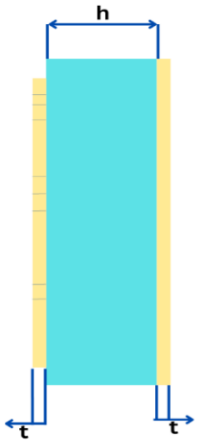

Fig.2 Diagrammatic representation of the side view of a polarization converter unit.

3. ANALYSIS AND DISCUSSION

The present study involves the development and simulation of a polarization converter using CST Microwave Studio, an electromagnetic software. The solver employed for the simulation is based on frequency domain analysis, and it implements the finite element algorithm.

The simulation's x and y axes are confined by unit cell boundary criteria, but its z axis is constrained by open add space boundary conditions. A linearly polarised electromagnetic pulse with an x-orientation is used to turn on the converter by illuminating the topmost metallic pattern layer from the negative z-axis. When the incident wave is x-polarized, two reflection coefficients are defined: the co-polarization reflection coefficient (r_{xx}) and the cross-polarization reflection coefficient (r_{yx}). The expressions for these coefficients are listed below.

$$r_{xx} = E_{rx} / E_{ix} \quad (1)$$

$$r_{yx} = E_{ry} / E_{ix} \quad (2)$$

(a)

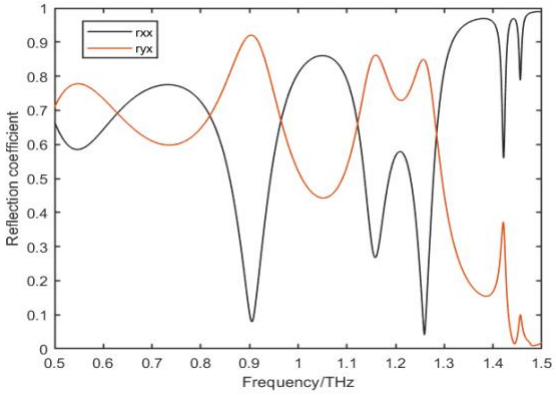

(b)

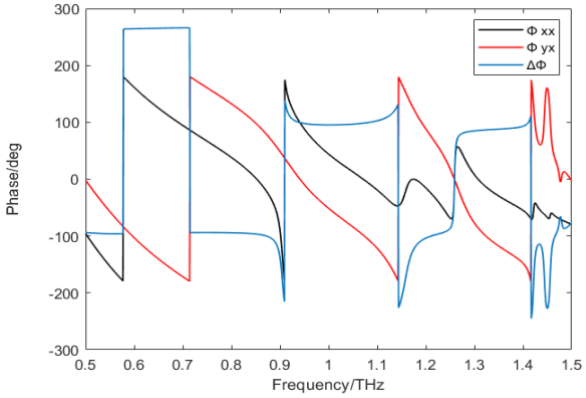

Fig.3 Reflection of the polarisation converter under co- and cross-polarization. (a)Coefficient, (b) Phase.

The reflection coefficient, r_{ij}, is used to describe the reflection of the j-polarized wave into the i-polarized wave. E_{ry} stands for x- and y-directions reflected electric fields, respectively. Similar to each other, the letters E_{rx} and E_{ry} stand for the incident electric fields in the x- and y-directions. Below is a description of the polarisation conversion ratio (PCR) of the reflective metasurface polarisation converter.

$$PCR = \frac{|r_{yx}|^2}{|r_{yx}|^2 + |r_{xx}|^2} \quad (3)$$

The reflecting converter's ellipticity equations can be obtained using the Stokes equations in optics.

$$S_0 = r^2_{xx} + r^2_{yx} \quad (4)$$

$$S_1 = r^2_{xx} - r^2_{yx} \quad (5)$$

$$S_2 = 2r_{xx}\, r_{yx} \cos \delta \quad (6)$$

$$S_3 = 2r_{xx}\, r_{yx} \sin \delta \quad (7)$$

Where $\delta = \Phi_x - \Phi_y$ is the phase difference between r_{xx} and r_{yx}, whereby the ellipticity formulas can be derived:

$$Ellipticity = S_3 / S_0 \quad (8)$$

(a)

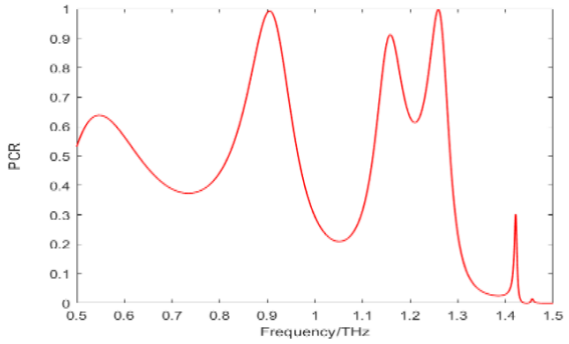

(b)

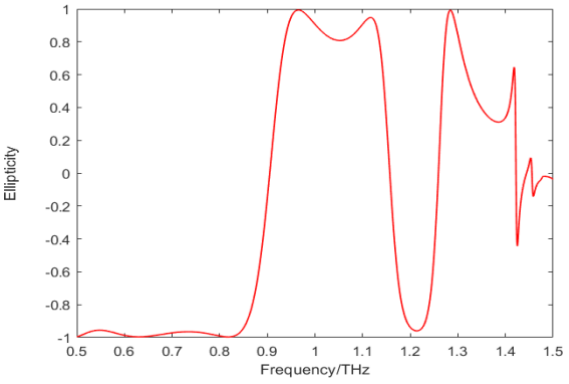

Fig.4 Reflected waves impact on reversed wave waves (a) polarisation conversion rate (PCR) (b) the reversed wave's ellipticity.

The coefficient and phase values for the converter's reflection qualities under an x-polarization wave's illumination are shown in Fig. 3. In the three bands of 0.87260.8924 THz, 1.10751.1147 THz, and 1.26141.2731 THz, the cross-polarization coefficient r_{yx} is larger than 0.85 and the co-polarization coefficient r_{xx} is less than 0.3. This demonstrates successful LCP conversion and the converter's PCR is greater than 95%, as shown in Fig. 4(a). Also, for the three bands of 0.516~0.862 THz, 0.947~0.986 THz, and 1.9861.203 THz, respectively, the co- and cross-polarization coefficients have comparable values ($r_{xx} \approx r_{yx}$) and a phase difference ($\Delta\Phi$) of $\pm 90^\circ \pm 10^\circ$ or $\pm 270^\circ \pm 10$. The converter's ellipticity can be computed using Eqs. (4) through (8), as shown in Fig. 4(b). The ellipticity can be demonstrated to be close to ±1, with "+" and "-" standing for RHCP and LHCP, respectively, and "+" and "-" designating the bands where LTCP conversion has been achieved.

The dual-functional terahertz metasurface polarisation converter clearly outperforms other designs in a variety of ways when compared to the most recent metasurface polarisation converter, as shown in Table 1. In terms of operational effectiveness, polarisation conversion ratio (PCR), maximum linear-to-circular polarisation (LTCP) conversion bandwidth (FBW), and ellipticity of reflected waves, it performs better than rivals. Moreover, a wide range of angular stability is shown. Moreover, the suggested converter incorporates an easy-to-fabricate top metal pattern layer. Last but not least, this work introduces a novel design approach that has not previously been reported, combining structures with varied pattern structures and those with various sizes in the u and v directions to achieve multiband and multifunction polarisation conversion. The knowledge offered by this design plan may be very useful in developing future metasurface polarisation converter designs.

Table 1

Analysing the proposed structure in light of previous converters that have been described.

References	Polarization properties	Operation Frequency	Eilli.	PCR	Angular stability
Pan W [12]	Cross	0.58~1.35 THz	NIL	85%	30˚
Jiang Y [11]	Circular	0.60~1.41 THz	0.8	NIL	20˚
Dutta R [15]	Cross Circular	4.3,7.2,12.3,15.15 GHz 4.75~5.95, 8.35~8.8 GHz	NIL 0.9	90% NIL	15˚
Bilal H [18]	Cross Circular	1.10,2.13,3.46 THz 1.20~1.83,2.52~3.10, 3.78~3.90 THz	NIL 0.8	90% NIL	20˚
This work	Cross Circular	0.87~ 0.89,1.10~1.11,1.26~1.27 THz 0.51~0.86,0.94~0.98,1.98~1.20 THz	NIL 0.96	95% NIL	50˚

4. CONCLUSION

Finally, a proposal for a multi-band, dual-functional metasurface terahertz polarization converter built on three asymmetric Jerusalem cross structures. The recommended converter displays LCP behavior in a range of three frequencies between 0.8726~0.8924 THz, 1.1075~1.1147THz, and 1.2614~1.2731THz. The PCR of the converter is greater than 95% in these two operational bands, and the ellipticity of the reflected wave is nearly zero. Additionally, at three bands of 0.516~0.862 THz, 0.947~0.986 THz, and 1.986~1.203 THz, the suggested converter exhibits LTCP converter behavior. Within these three operational bands, the reflected wave's ellipticity gets closer to 1. Surface current and the theory of multiple interference are used to examine the physical mechanism of polarization conversion. The suggested converter's function, PCR, and ellipticity are all significantly superior than those of the earlier polarization converters. Also, the converter's straightforward top metal pattern makes it manifest for a variety of applications in addition to making it simple to build. Future designs of metasurface polarization converters can benefit from some reference experience provided by this technology. The terahertz polarization converter that is being proposed can be effectively employed in terahertz communication, imaging, and sensing.

AUTHOR CONTRIBUTION: We declare equal contribution from all the authors.

FUNDING: The authors declare that no funds, grants, or other support were received during the preparations of this manuscript.

DECLARATIONS:

ETHICS APPROVAL: There is no ethical approval required. Not applicable. Consent to Participate Informed consent was obtained from all individual participants included in the study. Not applicable.

CONSENT FOR PUBLICATION: Authors are responsible for the correctness of the statements provided in the manuscript.

CONFLICT OF INTEREST: The authors declare no competing interests.

DATA AVAILABILTY: Data will be provide upon request to the authors.

5. REFERENCES

[1] Q. Wang, L. Xie, Y. Ying, Overview of imaging methods based on terahertz time-domain spectroscopy, Appl. Spectrosc. Rev. 57 (3) (2022) 249–264.

[2] I. Malhotra, K.R. Jha, G. Singh, Terahertz antenna technology for imaging applications: A technical review, Int. J. Microw. Wirel. Technol. 10 (3) (2018) 271–290.

[3] Y. Zhang, C. Wang, B. Huai, et al., Continuous-wave THz imaging for biomedical samples, Appl. Sci. 11 (1) (2020) 71.

[4] J. Hao, Q. Ren, Z. An, et al., Optical metamaterial for polarization control, Phys. Rev. A 80 (2) (2009) 023807.

[5] L.H. Nicholls, F.J. Rodríguez-Fortuño, M.E. Nasir, et al., Ultrafast synthesis and switching of light polarization in nonlinear anisotropic metamaterials, Nat. Photonics 11 (10) (2017) 628–633.

[6] S. Zhang, Z. Li, F. Xing, Review of polarization optical devices based on graphene materials, Int. J. Mol. Sci. 21 (5) (2020) 1608.

[7] D. Wang, Y. Gu, Y. Gong, et al., An ultrathin terahertz quarter-wave plate using planar babinet-inverted metasurface, Opt. Express 23 (9) (2015) 11114–11122

[8] C.L. Holloway, E.F. Kuester, J.A. Gordon, et al., An overview of the theory and applications of metasurfaces: The two-dimensional equivalents of metamaterials, IEEE Antennas Propag. Mag. 54 (2) (2012) 10–35.

[9] Q. He, S. Sun, S. Xiao, et al., High-efficiency metasurfaces: principles, realizations, and applications, Adv. Opt. Mater. 6 (19) (2018) 1800415.

[10] G. Moon, J. Choi, C. Lee, et al., Machine learning-based design of meta-plasmonic biosensors with negative index metamaterials, Biosens. Bioelectron. 164 (2020) 112335.

[11] Y. Jiang, L. Wang, J. Wang, et al., Ultra-wideband high-efficiency reflective linear-to-circular polarization converter based on metasurface at terahertz frequencies, Opt. Express 25 (22) (2017) 27616–27623.

[12] W. Pan, X. Ren, Q. Chen, A terahertz quarter wave plate based on staggered split ring resonators, Prog. Electromagn. Res. Lett. 85 (2019) 117–123.

[13] Z. Song, J. Zhang, Achieving broadband absorption and polarization conversion with a vanadium dioxide metasurface in the

same terahertz frequencies, Opt. Express 28 (8) (2020) 12487–12497.

[14] Z. Li, R. Yang, J. Wang, et al., Multifunctional metasurface for broadband absorption, linear and circular polarization conversions, Opt. Mater. Express 11 (10) (2021) 3507–3519.

[15] R. Dutta, J. Ghosh, Z. Yang, et al., Multi-band multi-functional metasurface-based reflective polarization converter for linear and circular polarizations, IEEE Access 9 (2021) 152738-152748.

[16] F. Hao, J. Zang, Design of a butterfly shaped reflective multifunctional po-larization converter, in: 2022 IEEE 5th International Conference on Electronic Information and Communication Technology, ICEICT, IEEE, 2022, pp. 523–525.

[17] J.S. Li, F.Q. Bai, Dual-band terahertz polarization converter with high-efficiency asymmetric transmission, Opt. Mater. Express 10 (8) (2020) 1853–1861.

[18] R.M.H. Bilal, M.A. Baqir, P.K. Choudhury, et al., On the specially designed fractal metasurface-based dual-polarization converter in the THz regime, Results Phys. 19 (2020) 103358.

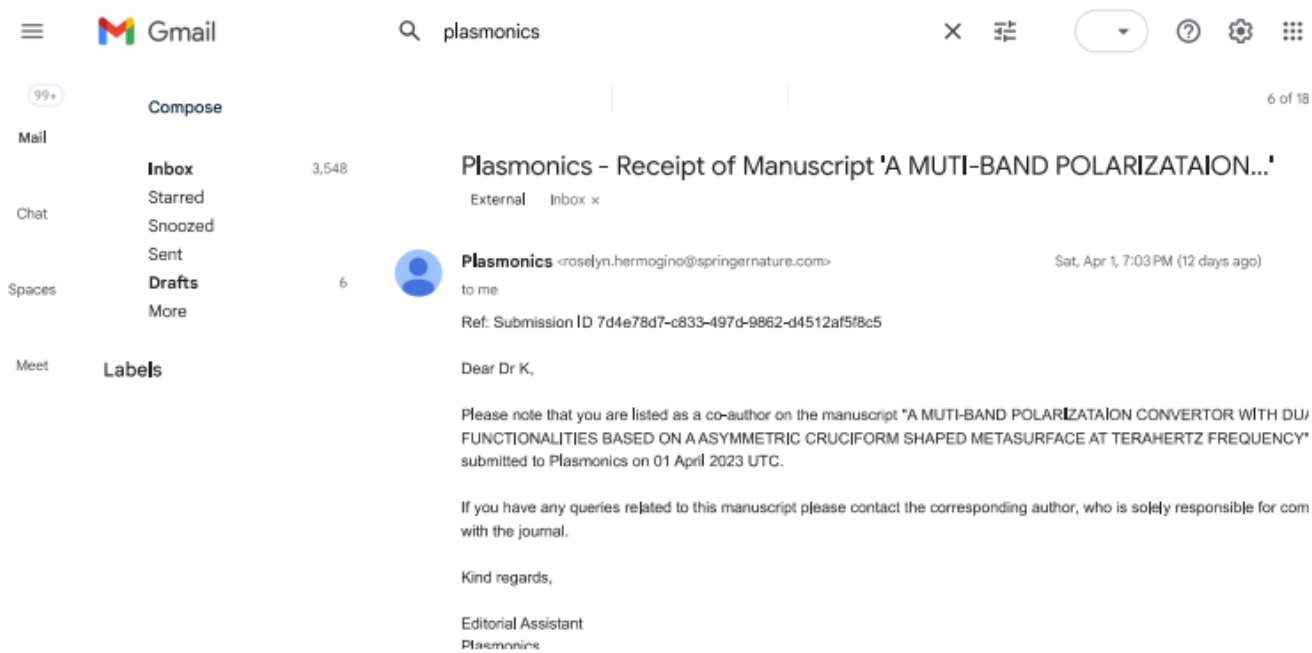
Gmail
plasmonics
99+
Mail
Chat
Spaces
Meet
Compose
Inbox 3,548
Starred
Snoozed
Sent
Drafts 6
More
Labels
6 of 18
Plasmonics - Receipt of Manuscript 'A MUTI-BAND POLARIZATAION...'
External
Inbox ×
Plasmonics <roselyn.hermogino@springernature.com>
Sat, Apr 1, 7:03 PM (12 days ago)
to me
Ref: Submission ID 7d4e78d7-c833-497d-9862-d4512af5f8c5
Dear Dr K,
Please note that you are listed as a co-author on the manuscript "A MUTI-BAND POLARIZATAION CONVERTOR WITH DU
FUNCTIONALITIES BASED ON A ASYMMETRIC CRUCIFORM SHAPED METASURFACE AT TERAHERTZ FREQUENCY"
submitted to Plasmonics on 01 April 2023 UTC.
If you have any queries related to this manuscript please contact the corresponding author, who is solely responsible for com
with the journal.
Kind regards,
Editorial Assistant
Plasmonics